Biomaterials Advances 153 (2023) 213526

Contents lists available at ScienceDirect

Biomaterials Advances

journal homepage: www.journals.elsevier.com/materials-science-and-engineering-c

Microneedle array patches for sustained delivery of fluphenazine: A micron scale approach for the management of schizophrenia

Juhaina M. Abu Ershaid [a,b], Lalitkumar K. Vora [a], Fabiana Volpe-Zanutto [a,c], Akmal H. Sabri [a], Ke Peng [a], Qonita K. Anjani [a], Peter E. McKenna [a], Anastasia Ripolin [a], Eneko Larrañeta [a], Helen O. McCarthy [a], Ryan F. Donnelly [a,*]

[a] School of Pharmacy, Queen's University Belfast, 97 Lisburn Road, Belfast BT9 7BL, UK
[b] School of Pharmacy, Department of Applied Pharmaceutical Sciences and Clinical Pharmacy, Isra University, Amman 11622, Jordan
[c] Faculty of Pharmaceutical Sciences, R. Cândido Portinari, 200 - Cidade Universitária, Campinas, SP 13083-871, University of Campinas, Brazil

ARTICLE INFO

Keywords:
Microneedles
Antipsychotic
Hydrophobic
Controlled release
Nanoemulsion
PLGA

ABSTRACT

Schizophrenia is a severe chronic mental illness characterised by impaired emotional and cognitive functioning. To treat this condition, antipsychotics are available in limited dosage forms, mainly oral and injectable formulations. Although injectable antipsychotics were designed to enhance adherence, they are invasive, painful and require a healthcare professional to be administered. To overcome such administration issues, extensive research has been focused on developing transdermal antipsychotic formulations. In this work, three microneedle (MN) systems were developed to deliver fluphenazine (FLU) systemically. A decanoic prodrug of FLU called fluphenazine decanoate (FLU—D) was used in two of the MN formulations due to its high lipophilicity. FLU-D was loaded into dissolving MNs and nanoemulsion (NE)-loaded MNs. The parent drug FLU was loaded into poly(lactic-*co*-glycolic acid) (PLGA)-tipped MNs. All MN systems were characterised and evaluated *in vitro* and *in vivo*. The *in vivo* evaluation of the three developed MN systems showed their ability to deliver FLU into the systemic circulation, as the C_{max} of FLU-D dissolving MNs was 36.11 ± 12.37 ng/ml. However, the C_{max} of FLU-D NE loaded dissolving MNs was 12.92 ± 6.3 ng/ml and for FLU-PLGA tipped MNs was 21.57 ± 2.45 ng/ml. Compared to an intramuscular (IM) injection of FLU-D in sesame oil, the relative bioavailabilities were 26.96 %, 21.73 % and 42.45 % for FLU-D dissolving MNs, FLU-D NE dissolving MNs and FLU-PLGA tipped MNs, respectively. FLU plasma levels were maintained above the minimum human therapeutic limits for a week. Consequently, these various MN formulations are considered to be a viable options for the transdermal delivery of fluphenazine and its prodrug. The three MN systems developed offer patients a user-friendly, painless, and convenient long-acting delivery method for FLU. Reducing dosing frequency and using less invasive drug administration methods can enhance adherence and foster positive therapeutic outcomes. This study demonstrates the capability and adaptability of MNs technology to transport hydrophobic molecules from the skin to the systemic circulation.

1. Introduction

Schizophrenia is a chronic psychiatric illness with undefined aetiology and pathology [1]. The diagnosis of schizophrenia is confirmed upon observation of symptoms, such as delusions, hallucinations or disorganised speech, which are present for a significant portion of time [2]. This mental disorder presents a massive obstacle not only for patients and their families but also for the healthcare system and the economy [3]. Mortality rates for patients with schizophrenia are two- to threefold greater than in the general population [4]. Similar to other severe mental disorders, schizophrenia treatment requires regular intake of medications, as prescribed, to prevent relapses, control symptoms and maintain treatment efficacy [5].

Long-term management is indeed challenging, as patients with schizophrenia frequently have poor medicine compliance that culminates in relapse and rehospitalisation [6]. In fact, studies report that up to 74 % of patients discontinue their medication within 18 months of starting a new antipsychotic therapy [7]. This can impose a significant

* Corresponding author at: School of Pharmacy, Queen's University Belfast, Medical Biology Centre, 97 Lisburn Road, Belfast BT9 7BL, UK.
E-mail address: r.donnelly@qub.ac.uk (R.F. Donnelly).

https://doi.org/10.1016/j.bioadv.2023.213526
Received 1 February 2023; Received in revised form 6 June 2023; Accepted 13 June 2023
Available online 15 June 2023

economic burden on the healthcare system. For instance, in the UK, the cost of a schizophrenic relapse to the National Health Service (NHS) due to medicine noncompliance can amount to £15,000/year/patient [8,9]. This can have severe financial repercussions due to the prevalence of the disease within the population. Therefore, medication adherence plays a substantial role in enhancing the overall clinical outcomes of the treatment while mitigating any unwanted consequence of medicine adherence. Currently, antipsychotics used for the treatment of schizophrenia are delivered either orally or as injectable formulations. The requirement for frequent administration with oral antipsychotics highly impacts patients' day-to-day routine, which coupled with inadvertent causes such as forgetfulness and attitude towards the disease, culminates in poor adherence [10]. Given these limitations, there is a paradigm shift towards administering antipsychotics *via* long-acting injectables as a means to reduce dosing frequency while improving compliance and clinical outcome [11]. Long-acting intramuscular injectables obviate the issues of poor bioavailability, as the drug is directly delivered into systemic circulation, thus avoiding hepatic first-pass metabolism [12]. In addition, these formulations are also beneficial in cases where patients refuse to swallow or adhere to oral medications. Nevertheless, this route of administration is not only invasive and painful but also necessitates the assistance of healthcare professionals in administering the formulation, which imposes additional intangible and direct costs to the overall treatment. In addition, the painful nature of injecting these formulations intramuscularly may compromise the relationship between patients and healthcare professionals [13–15].

Owing to the limitations of oral antipsychotics and intramuscular injections, there has been an impetus to explore alternative routes of administration that can improve the bioavailability of the delivered antipsychotic in a minimally invasive fashion with the aim of improving patient compliance and overall treatment outcomes. Recently, a transdermal patch that delivered the antipsychotic blonanserin was approved in Japan. This formulation conferred stable blood concentrations of the drug over long periods by circumventing first-pass hepatic metabolism that can affect plasma levels of oral antipsychotic agents [16]. However, delivering molecules across the skin using conventional transdermal patches is highly dependent on the physiochemical properties of the delivered molecules. To ensure efficient permeation through the different strata of the skin, the molecules should have molecular weights $<$600 Da with log *P* values between 1 and 3. In addition, molecules should be soluble in aqueous media with high partitioning ability to diffuse out of the patch and move across the *stratum corneum* (*SC*) [17]. Given these strict physiochemical requirements, there is a narrow spectrum of drug molecules that can be delivered *via* conventional transdermal patches. Nevertheless, the capability to deliver blonanserin highlighted that delivering antipsychotics *via* the transdermal route may offer an elegant solution to improve compliance in a minimally invasive manner.

One transdermal drug delivery system that has yet to be fully explored for the delivery of antipsychotic agents is microneedles (MNs) [16,18]. These are minimally invasive transdermal delivery systems that augment the delivery of therapeutic agents transdermally by overcoming the physical barrier function of the skin [19,20]. Upon skin application, MNs bypass the *SC* to deliver the therapeutic agent to the dermal microcirculation, which eventually reaches the systemic circulation [21–23]. In tandem with unprecedented progress within the field of polymer chemistry over the decades, MN technology has recently been investigated as a potential drug delivery platform to confer a sustained drug release profile following a single patch application [24–26]. Such a sustained release profile of the delivered therapeutic is achievable by judicious selection of the polymeric excipient in combination with meticulous selection in the overall design of the MN system that culminates in precision control over polymer degradation upon skin application [27,28]. Therefore, adjusting the molecular weight or the molar ratio of the polymeric excipient modifies drug release [29,30]. In addition, an additional level of control over drug release can be incorporated into the pharmaceutical system by first loading the payload into nanoparticle preparations such as liposomes, solid lipid nanoparticles and nanocrystals, which are then loaded into the MN system [21,31,32]. Nevertheless, such delivery strategies have yet to be explored for the delivery of antipsychotic agents.

In this work, we present for the first time the use of MN technology for the delivery of the highly hydrophobic drug fluphenazine decanoate (FLU—D) across the skin. FLU-D is a viscous liquid that has a low melting point of approximately 30 °C and a molecular weight of 591.77 g/mol with log *P* 7.25 [33]. These physiochemical properties preclude the delivery of the drug using conventional transdermal patches. Therefore, we explored the utility of MN-based delivery systems as a means to administer the antipsychotic agent in a minimally invasive fashion. In this work, we investigated the effect of different variants of dissolving MN systems on the delivery of the encapsulated drug. First, a simple casting technique was employed to prepare dissolving MNs loaded with the prodrug FLU—D. This MN formulation was fabricated from the water-soluble and biocompatible polymers PVP and PVA. Second, the combination of nanoparticulate systems with MN technology was also investigated as a potential strategy to prolong the release profile of the drug over a prolonged period of several weeks. This was achieved by first fabricating a nanoemulsion of FLU-D using a quality by design (QBD) approach loaded into a dissolving MN formulation. Finally, implantable-based dissolving MNs were also investigated by preparing FLU-PLGA tipped MNs. All three MN systems were evaluated *in vitro* before proceeding into a pharmacokinetic study *in vivo* using a rat model. The composite MN systems developed in the current work may offer a patient-friendly approach to administer the antipsychotic agent FLU transdermally in a painless fashion over a sustained period for the management of schizophrenia.

2. Materials and methods

2.1. Materials

Acetonitrile for high-performance liquid chromatography (HPLC), ammonium acetate, methanol for HPLC, bovine serum albumin (BSA), poly(vinyl alcohol) (PVA) (MW 10 kDa and 31–50 kDa), Tween®80, Tween®20, Pluronic®L-31 (PL®31), Pluronic®L-64 (PL®64), Nile red, sodium dodecyl sulfate (SLS), formic acid, sesame oil and sucrose were purchased from Sigma–Aldrich (Dorset, UK). Glycerol (Anala Rnormapur, 99.5 %) was purchased from VWR International (Leicestershire, UK). Fluphenazine decanoate was obtained from Manus Aktteva Biopharma (Gujarat, India). Disposable razor (Gillette Blue IITM, Gillette, Reading, UK). Poly(lactic-*co*-glycolic acid) (PLGA), a 50:50 M ratio of lactide:glycolide, inherent viscosity: 0.59 dl/g, Durect, Cupertino, (California, USA). Poly(vinyl pyrrolidone) (PVP) (MW 29–32 kDa), Ashland, (Kidderminster, UK). Dimethyl sulfoxide (DMSO) was provided by VWR International Limited (Leicestershire, UK). Piglets were provided by the Agri-Food and Bioscience Institute (Hillsborough, Northern Ireland, UK). Sodium hyaluronate was provided by Kewpie Corporation Shibuya-Ku (Tokyo, Japan). Fluphenazine hydrochloride was purchased from Chemos Sonnenring (Aldrich, Germany). Uranyl acetate was purchased from Ted Pella (Redding, USA). All other reagents were of analytical grade and purchased from standard commercial suppliers.

2.2. In vitro and in vivo analytical analysis

For in vitro studies, FLU and FLU-D amounts were determined using a validated dual detection HPLC method described previously [34] with slight modifications. Ultraviolet (UV) detection was used in this method. The analysis of the in vivo samples was performed using an HPLC-mass spectrometry (MS) method containing a quaternary pump, multisampler, and multicolumn thermostat equipped with an atmospheric pressure chemical ionisation (APCI) source (API 6400, Agilent

Technologies, UK) operated in positive electrospray ionisation mode [35]. The detection was measured by single ion monitoring (SIM) at 438.2 m/z. The HPLC–MS chromatographic conditions are outlined in the supplementary data.2.3 Formulation and optimisation of FLU-D NE.

First, FLU-D was mixed with PL®64 and sesame oil using a speed mixer at 6000 × g for 10 min until complete solubilisation of the drug in sesame oil to form a homogenous oily phase. The aqueous phase was composed of an aqueous blend of 18 % *w*/w PVA 10 kDa in deionised water. Furthermore, the oily phase was transferred to the aqueous phase using a 1 ml syringe dropwise under sonication using a probe sonicator (Amplitude of 80 % (71 W) with 10 s pulse on and 5 s pulse off) [36]. In this study, four surfactants (Tween®80, Tween®20, PL®31 and PL®64) were screened based on the saturation solubility of FLU-D in surfactant solutions with sesame oil. The surfactants were added to the nano-emulsion in order to stabilise the system. In addition, PVA and PEG were also screened as cosurfactants based on the NE droplet morphology and size. Cosurfactants are chemical entities typically comprised of short-chain amines or alcohols that are added in the presence of surfactant to aid in lowering the interfacial tension between the oil phase and the aqueous phase. By lowering the surface tension of the two phases under agitation, the presence of co-surfactants within a colloid promotes the emulsification and stabilisation of the system [37]. The NE formulation was optimised using a four-factor, five-level central composite design (CCD) with Design Expert® Software version 11 (State-ease, Minneapolis, USA). The oil amount, surfactant:oil ratio (SOR), cosurfactant amount and sonication time were used as variable factors in the optimisation process. Two responses were then recorded, namely, droplet size and polydispersity index (PDI).

2.3. Characterisation, release and stability of the optimised FLU-D NE

FLU-D NE was characterised in terms of particle size and PDI using a NanoBrook Omni particle sizer analyser (Brookhaven, New York, USA). The percentage of encapsulation efficiency (EE%) and loading capacity (LC%) were determined using the ultracentrifugation method with an Amicon® Ultra Centrifugal Device (Millipore Inc., molecular weight cut-off (MWCO) of 12 kDa) as this procedure provide a simple, fast and effective way to measure encapsulation efficiency. The amount of unencapsulated FLU-D was determined using the validated UV-HPLC analytical method. Eqs. (1) and (2) were used to calculate the EE% and LC% of FLU-D NE, respectively [38].

$$EE\% = \frac{Qtotal - Qfree}{Qtotal} \times 100\% \quad (1)$$

where Q total is the total amount of FLU-D in the formulation and Q free is the amount of unencapsulated FLU-D in the NE.

$$LC\% = \frac{Qtotal - Qfree}{Qcub} \quad (2)$$

where Q cub is the amount of all the components of the NE, Q total is the total amount of FLU-D in the formulation and Q free is the amount of unencapsulated FLU-D in the NE.

Morphological characterisation of FLU-D NE was carried out using transmission electron microscopy (TEM) (JEM-1400 Plus; JEOL, Tokyo, Japan). Urinal acetate was used as a staining agent. One drop of FLU-D NE was placed on top of a carbon grid, and a drop of 2 % urinal acetate in water was added. The carbon grids were left to dry overnight at room temperature (RT) [21]. A physical stability study of FLU-D NE in terms of droplet size and PDI was conducted under two different storage conditions (RT and 4 °C). The *in vitro* release of FLU-D from NE was inspected using the dialysis bag method [39]. The study was conducted using pure FLU-D and FLU-D NE, which were dispersed into the dialysis membrane. Dialysis bags were embedded in 100 ml of the release media (0.1 % *w*/w BSA and 1 % w/w SLS in PBS) at 37 °C in a water bath at 22 g. SLS was added to enhance the aqueous solubility of FLU-D in PBS, and BSA was added to enhance FLU-D stability in aqueous media to allow inspection of the drug release. The use of BSA as a drug stabiliser in solution has been reported before [40]. At predetermined time points, 1 ml of the release media was taken and replaced with 1 ml of fresh release media to maintain the sink condition. The FLU-D amount in the release media at each time point was quantified using the previously validated dual detection HPLC method.

2.4. MN formulation

FLU-D NE MNs were developed using the following steps, FLU-D NE was added to 40 % *w*/w PVP 58 kDa aqueous solution and mixed using a Speedmixer® for 3 min at 6000 g to form the first layer of MNs. Furthermore, the NE-PVP blend was cast into MNs moulds (600 pyramidal MNs per array, with area of 0.75 cm^2 and 750 μm MNs heights) and 5 bar pressure was applied using a pressure chamber. Then, MNs were centrifuged at 1000 ×*g* for 10 min. The excess formulation was removed, and MNs were left to dry at RT for 24 h. Finally, MNs baseplate (BP), was made of an aqueous blend of 15 % *w*/w PVA 31–50 kDa with 20 % *w*/w PVP 29–32 kDa. BP was cast into the MN moulds (600 pyramidal MNs per array, with area of 0.75 cm^2 and 750 μm MNs heights), centrifuged at 6000 ×*g* for 5 min and left to dry for 24 h at RT as detailed in Fig. 1 (A). For FLU-D dissolving MNs, FLU-D was loaded directly into an aqueous blend of polymers (20 % w/w PVA 10 kDa: 20 % w/w PVP 29–32 kDa) and mixed using Speedmixer® for 15 min at 6000 g. The drug-polymer mixture was cast into MNs moulds (600 pyramidal MNs per array, with area of 0.75 cm^2 and 750 μm MNs heights), and a pressure of 5 bar was applied for 15 min using the pressure chamber. Then, the excess of the formulation was removed, and MNs were left to dry at RT for 24 h. For the drug-free BP, an aqueous blend of 1.5 % *w*/w glycerol in 50 % w/w PVP 50 kDa was poured and centrifuged at 6000 ×*g* for 15 min, and then MNs were left to dry at RT for 24 h as outlined in Fig. 1 (B). To prepare FLU-PLGA tipped MNs, the tips were made of a solution of FLU and PLGA in a ratio of 75:25 dissolved in DMSO, as shown in Fig. 1 (C). To fill all the tips in the moulds (600 pyramidal MNs per array, with area of 0.75 cm^2 and 750 μm MNs heights), 80 μl of the tips solution were cast in the moulds. Followed by centrifugation at 10,000 ×*g* for 10 min, the excess solution was removed, and the moulds (600 pyramidal MNs per array, with area of 0.75 cm^2 and 750 μm MNs heights) were dried at RT for 4 h (this step was performed twice). The multicasting approach was used as described previously [41]. As a separating layer between FLU-PLGA tips and the BP, 100 mg of sodium hyaluronate and 25 mg of sucrose were dissolved in 10 ml water and cast in the MN moulds (600 pyramidal MNs per array, with area of 0.75 cm^2 and 750 μm MNs heights). The moulds (600 pyramidal MNs per array, with area of 0.75 cm^2 and 750 μm MNs heights) were centrifuged at 6000 ×*g* for 3 min. The excess of the separating layer was removed, and an aqueous blend of 15 % *w*/w PVA 31–50 kDa and 20 % w/w PVP 29–32 kDa was added and centrifuged for 3 min at 6000 *g* to form the BP. Finally, MNs were left to dry at RT for 24 h.

2.5. Mechanical and insertion properties evaluation of the three MN systems

The three MN systems were evaluated in terms of their mechanical and insertion properties using compression tests and Parafilm®M insertion tests using a TA-X2 Texture Analyser (Stable Microsystem, Haslmere, UK) [42–44]. Eq. (3) was used to calculate the percentage of height reduction following the compression force test on MNs.

$$Height\ reduction\% = \frac{Hb - Ha}{Hb} \times 100\% \quad (3)$$

where Hb is the MN length before applying the compression force test and Ha is the MN length after applying the test.

The commercial polymeric film Parafilm®M was evaluated as a

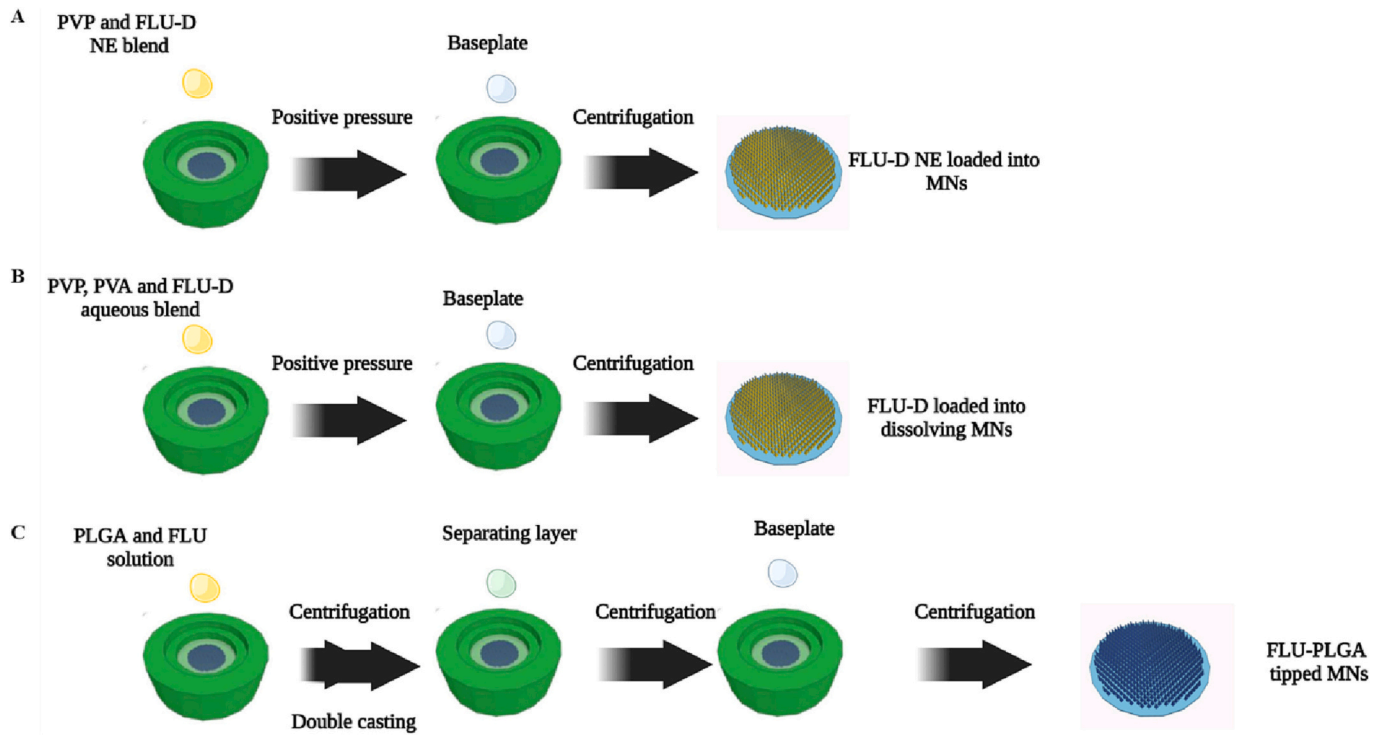

Fig. 1. A schematic representation showing **A:** The preparation method of FLU-D NE loaded into MNs. **B**: The preparation method of FLU-D loaded dissolving MNs **C:** The preparation method of FLU-PLGA tipped MNs.

model membrane for MN insertion studies. The insertion test was performed using the Texture Analyser, and a sheet of Parafilm®M was folded into eight layers with a total thickness of approximately 1 mm. The MNs were attached to the movable cylindrical probe of the Texture Analyser, which was programmed to move downwards at a speed of 0.5 mm/s until it reached the Parafilm®M layers to apply a force of 32 N/array for 30 s in a compression mood. Holes created in each layer were counted under the stereomicroscope. The percentage of holes created in each layer was calculated using Eq. (4).

$$Holes\ created\% = \frac{Number\ of\ holes\ in\ each\ layer}{Total\ number\ of\ MNs} \times 100\% \quad (4)$$

2.6. FLU in vitro release from FLU-PLGA tipped MNs

FLU-PLGA tipped MNs were placed in 4 ml of the release media (0.1 % *w*/w BSA in 1 % w/w SLS in PBS). Samples were kept at 80 rpm at 37 °C in a water bath covered with aluminium foil. At predetermined time points (1, 2, 3, 4, 7, 14 and 21 days), samples were taken, diluted and filtered before being injected into the HPLC. At each time point, the same volume of sample was replaced with fresh release media [41].

2.7. Ex vivo skin deposition of the three developed MN systems

The FLU-D content in each of the FLU-D dissolving MNs and FLU-D NE dissolving MNs was quantified by dissolving the MNs in the release media (0.1 % *w*/w BSA in 1 % w/w SLS in PBS) until complete dissolution. Samples were diluted and vortexed for 15 min and then centrifuged at 14,000 ×*g* for 15 min. Supernatants were collected and analysed using HPLC. The FLU content in the FLU-PLGA-tipped MN formulations was evaluated by dissolving the MNs in DMSO and sonicating them for 30 min. The solution was centrifuged at 14,000 ×*g* for 10 min. Supernatants were collected and analysed using the prescribed HPLC method. *An ex vivo* skin deposition study was carried out using a modified Franz diffusion cell apparatus, as described previously [14], using full-thickness neonatal porcine skin. The skin was obtained from stillborn piglets provided by the Agri-Food and Bioscience Institute (Hillsborough, Northern Ireland, UK). The piglets were immediately frozen after birth at −20 °C and defrosted overnight before use. Full-thickness skin was excised using a surgical scalpel and carefully shaved using a disposable razor (Gillette Blue IITM, Gillette, Reading, UK). Before the experiment, the skin samples were shaved and pre-equilibrated in PBS pH 7.4 for 30 min and then attached to the Franz diffusion cells using cyanoacrylate® glue.

In the receiver compartment, 12 ml of the release media (1 % *w*/w SLS in PBS (pH 7.4)) was used. The receiver compartment was stirred at 130 g and was thermostatically maintained at 37 ± 1 °C. The donor compartments and sampling arm were sealed using Parafilm®M. MNs were then inserted into the skin using manual force for 30 s, and a cylindrical stainless steel weight of 5.0 g was placed on top to ensure that MNs remained in place for the duration of the experiment. To quantify the FLU-D amount in skin sections, 300 μl of methanol was added, and each sample was vortexed for 30 min to dissolve the drug. Samples were centrifuged at 14,000 ×*g* for 15 min, and the supernatants were collected and analysed using the HPLC method.

2.8. In vivo studies of the three developed MN systems

The *in vivo* pharmacokinetic study of FLU was approved by the committee of the biological services unit, Queen's University Belfast. The study was conducted under procedure Project Licence number PPL 2903. Researchers who performed the procedure have Personal Licence numbers PIL1892, 2058, 2059, 2127, according to the policy of the Federation of European Laboratory Animal Science Associations and the European Convention for the Protection of Vertebrate Animals used for Experimental and Other Scientific Purposes, with the implementation of the principles of the 3Rs (replacement, reduction and refinement). In total, there were 30 Sprague Dawley rats, and the rats had a mean age of 9–11 weeks and a mean weight of 249.72 ± 13 g at the start of the study. They were acclimatised to laboratory conditions for a minimum of seven days before the experiment. The rats were divided into five groups, and

each group had ($n = 6$ rats): Group 1) oral FLU suspension (oral control) – each rat was given oral FLU suspension by oral gavage at a dose of (5 mg/kg), Group 2) IM injection of FLU-D (IM control) – each rat was given an IM injection of FLU-D in sesame oil (5 mg/kg), Group 3): FLU-D dissolving MNs – each rat received four MN arrays to achieve a dose of 20.64 mg/kg, Group 4): FLU-D NE dissolving MNs – each rat received four MN arrays to achieve a dose of 12.64 mg/kg and Group 5): FLU-PLGA tipped MNs – each rat received four MN arrays to achieve a dose of 9.12 mg/kg. To assess FLU pharmacokinetics, a 200 μl blood sample was taken from each rat at predetermined time points *via* tail vein bleed into heparinized (10 μl) Eppendorf tubes. The predetermined time points for the IM control and the three MN systems were 2 and 4 h ($n = 3$ for each time point) following the application or administration. For oral control, the time points were 0.4, 1, 2, 4 and 6 h ($n = 6$ for each time point) due to the short half-life of oral FLU. For all groups except the oral control, blood samples were taken on days 1, 2, 3, 4, 7 and 14 ($n = 6$ for each time point and from each group). For the oral FLU solution, the time points were 1, 2, 3 and 4 days ($n = 6$ for each time point), as rats were sacrificed on day 4 using a CO_2 chamber followed by cervical dislocation. Other rat groups were culled at the end of the study using a CO_2 chamber followed by cervical dislocation.

2.9. FLU extraction from plasma samples and pharmacokinetic parameter calculations

First, 100 μl of plasma sample was mixed with 300 μl of methanol, vortexed for 15 min for plasma protein precipitation and centrifuged at 14,000 $\times g$ for 15 min. The supernatants were transferred into glass inserts placed in HPLC vials to be analysed using the validated HPLC–MS method. Noncompartmental pharmacokinetic analysis of FLU plasma levels was performed using the PK Solver add-in program in Microsoft Office 365 ProPlus Excel [45]. Drug concentrations [ng/ml] were plotted against time [D]. The obtained pharmacokinetic parameters from PK Solver included the maximum plasma concentrations (C_{max}), the times of maximum plasma concentrations (t_{max}), the area under the curve ($AUC_{(0-7)}$) from time zero ($t = 0$) to the last experimental endpoint ($t = 7$), the mean half-life $t_{½}$ and the mean residence time (MRT). Relative bioavailability (F_{rel}) is a comparison between drug bioavailability obtained from two different formulations of the same drug. For FLU relative bioavailability, FLU bioavailability from the IM control was compared to FLU bioavailability obtained from dissolving MNs, NE-loaded MNs and FLU-PLGA-tipped MNs. FLU F_{rel} was calculated using Eq. (5).

$$FMNs = \frac{AUC\ MNs^{*}Dose\ control}{AUC\ control^{*}Dose\ MNs} \times 100\% \quad (5)$$

where AUC is the area under the curve obtained from PK Solver and Dose control is the drug dose that was given to each rat of the IM control group and dose [93].

2.10. Statistical analysis

All data were expressed as the means ± SDs, calculated using Microsoft Office 365 Pro Plus Excel (Microsoft Corporation, Redmond, WA, USA). Where appropriate, the Mann–Whitney test was used for the comparison of two groups. One-way ANOVA was used for the comparison of multiple groups. In all cases, $p < 0.05$ was considered a significant difference.

3. Results and discussion

3.1. Formulation and optimisation of FLU-D NE

Fluphenazine (FLU) is a phenothiazine derivative and one of the earliest drugs to be classified and approved by the United States Food and Drug Administration (USFDA) in 1959 as a typical antipsychotic. FLU is available as an oral formulation, and it is extensively metabolised by hepatic first pass metabolism, which significantly reduces the bioavailability of the drug [46]. Due to the frequent daily administration of the oral formulation, a prodrug of FLU was developed to minimise the dosing frequency and enhance the therapeutic outcomes. FLU was esterified with decanoic acid to form fluphenazine decanoate (FLU—D) [33]. FLU-D has a lower water solubility than the parent drug; therefore, it was dissolved in sesame oil and administered as an intramuscular injection (IM) every 2–4 weeks as a long-acting formulation [47]. Therefore, in this work, FLU-D was selected as the ideal candidate to achieve sustained drug delivery. To load this compound into MN arrays, nanoemulsions (NE) were formulated.

NE is an isotropic heterogeneous system where the drug is dispersed as nanodroplets within an immiscible liquid and stabilised by emulsifiers and co-emulsifiers [48]. Oil in water (O/W) NEs have been used as carriers to release lipophilic drugs [36], where the lipid or oily phase incorporates the lipophilic compounds and disperses them in the continuous aqueous phase [42]. NEs have several advantages over conventional emulsions, including stability and enhanced penetration. Because of the small droplet size and low surface tension between the oil and water molecules, they have a low potential to agglomerate or precipitate and reduce the possibility of creaming or sedimentation [49]. FLU-D hydrolyses to FLU by enzyme-mediated hydrolysis, which occurs in various parts of the body, including the injection sites, lymphatic system and blood. However, it was found that FLU-D hydrolysis following an injection of FLU-D in sesame oil is slow, mainly because of the ability of oil to protect the prodrug from esterases [50]. In this work, NE was used as a carrier of FLU-D to minimise the hydrolyses and extend the drug release.

Surfactants are amphiphilic structures composed of a hydrophilic group known as the head and a hydrophobic carbon chain known as the tail. Nonionic surfactants are preferred over anionic surfactants due to their lower toxicity and irritancy. Nanoemulsions are stabilised using surfactant or a mixture of surfactants. Previous studies have shown that steric interactions can be a main stabilising mechanism in emulsions formed from nonionic surfactants. Nanoemulsions must be stabilised against various physical instability mechanisms such as coalescence, ostwald ripening, and creaming [44,45].

In terms of formulating O/W emulsions, surfactants with hydrophilic lipophilic balance (HLB) values between 8 and 16 are usually used [53]. The first step was to evaluate the best surfactant to prepare a suitable NE that would be subsequently loaded into the MNs. The four selected nonionic surfactants showed a similar saturation solubility of FLU-D in sesame oil solution (Fig. 2 **(A)**). The ability of NE to keep the drug in the solubilised form depends on the drug solubility in the oily phase [54]. Surfactant screening based on their ability to enhance drug solubility in sesame oil was carried out to ensure maximum drug solubility in the oily phase. The oily phase in NE solubilises lipophilic molecules, leading to an enhancement in drug loading [52]. The difference ($p = 0.0931$) between the four screened surfactants in terms of saturation solubility was insignificant, as shown in Fig. 2 **(A).** Second, surfactants were screened based on the droplet size of NE prepared using each of them (Fig. 2 **(B)**). Droplet size has a significant effect on almost all the other properties of the emulsion, including physical stability, viscosity, *in vivo* efficacy and toxicity [55]. There was a significant difference ($p < 0.0001$) between the selected surfactants in terms of the droplet size of the NEs. NE prepared using PL®64 had the lowest droplet size compared to other NE prepared with the other surfactants. PL®64 was selected as the surfactant to prepare the optimised NE, as it helped in producing the lowest droplet size.

Cosurfactants are added to formulate a NE using the minimum surfactant concentration. Additionally, they increase the miscibility of oily and aqueous phases by partitioning between them [51]. The presence of cosurfactant decreases the bending stress of the interface and allows sufficient flexibility of the interfacial film to take up different curvatures

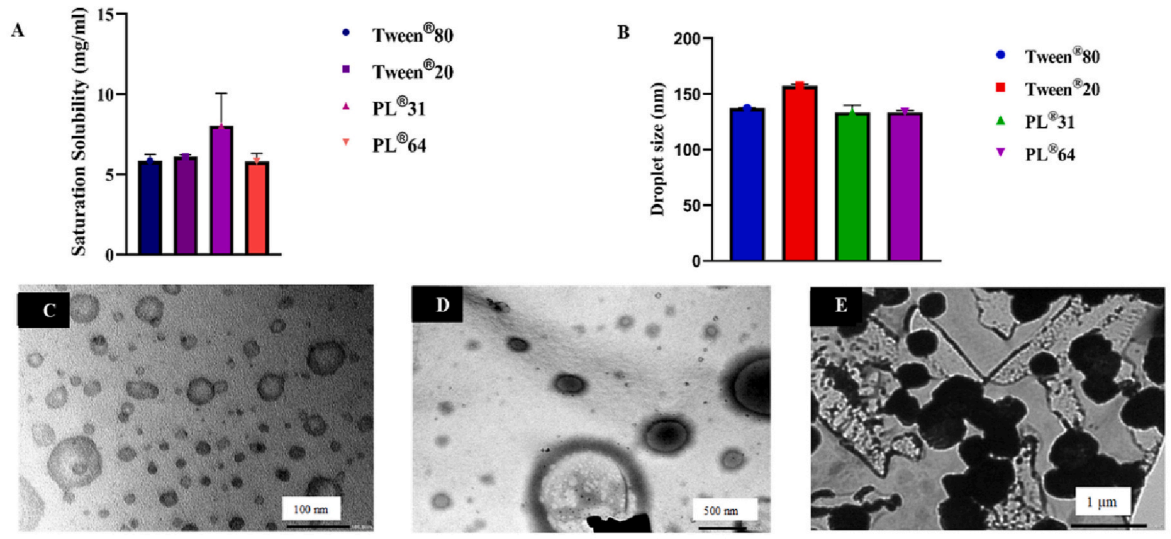

F. Droplet size and polydispersity index of nanoemulsions prepared with each of the selected co-surfactants (means ±S.D, n=3).

Co-surfactant	Droplet size (nm)	PDI
PVA 10 kDa	87.93 ± 1.2	0.18 ± 0.07
PEG 400	692.25 ± 15	0.17 ± 0.45

Fig. 2. Transmission electron microscope images of FLU-D NE prepared using Pluronic PL®64 as a surfactant and using each of the selected cosurfactants, **A:** PVA 10 kDa, **B:** PEG 400 and **C**: NE without cosurfactant. **D:** Surfactant screening based on drug solubility in surfactant solutions with sesame oil. **E:** Surfactant screening based on the droplet size of FLU-D NE prepared using each of the screened surfactants. Droplet sizes were measured using the particle sizer depending on DLS (means + S. D, $n = 3$). **F:** Droplet size and polydispersity index of NEs prepared with each of the selected cosurfactants (means ± S. D, $n = 3$).

required to form an NE over a wide range of compositions [56]. Fig. 2 **(F)** states the droplet size and PDI of NEs prepared using PL®64 as a surfactant with one of the selected cosurfactants (PVA 10 kDa and PEG 400). The PDI values of the two prepared NEs (PDI < 0.3) indicated the narrow distribution of droplet sizes [57]. TEM is widely used in visualising colloidal systems and their microstructures [58]. Based on the TEM image in Fig. 2 **(C)** and droplet size analysis, PVA 10 kDa was selected as a cosurfactant as a result of the uniform size and spherical shape of NE droplets. The morphologies of the NEs prepared using one of the two screened cosurfactants were also investigated using TEM. Fig. 2 **(D)** outlines TEM images showing clearly how the use of PEG 400 resulted in a wide variation in the droplet size of the NE. To demonstrate the effect of having a cosurfactant in the NE formulation, NE was prepared without a cosurfactant, where TEM images showed the irregular shape and aggregated droplets, as shown in Fig. 2 **(E).** The reported droplet size in our study is in line with a previously developed FLU NE [59]. In that work, the authors described a method to obtain FLU NE with particles ranging between 100 and 250 nm. The results are similar to those described in the present work. However, the method proposed is a complex methodology requiring up to 7 steps to prepare the NE, even requiring several pH changes over the process [59]. Therefore, the methodology proposed here is simpler. In addition to FLU NE, there are many other works described in the literature describing the use of microparticles for FLU drug delivery [60]. However, microparticles on their own cannot achieve high packing within MN arrays [61]. Therefore, NE and nanoparticles are preferably loaded into MN arrays.

To optimise the amount of each component and emulsification conditions, the quality by design (QBD) approach was applied by Design Expert® software. There is an emerging use of the QBD approach instead of trial and error to optimise pharmaceutical formulations. With this smart approach, several factors can be changed and investigated simultaneously [62]. The software provides 3D response surface plots that help in identifying the effect of variables on responses. Moreover, it offers a prediction of the optimum levels of each parameter for achieving the desired formulations [39]. A central composite design (CCD) was used to optimise the FLU-D NE formulation. Twenty-eight formulations were suggested from the software, and the responses of the dependent variables are demonstrated in the supplementary data. The results showed that the droplet sizes of the tested NE formulations were in the range of 75–1055.88 nm, and the PDI was between 0.10 and 0.32.

The results revealed that the droplet size and PDI of FLU-D NE followed quadratic models. The *F* value of droplet size analysis was 11.24. With respect to the PDI analysis, the *F* value was found to be 9.35. A *p* of <0.001 was found in the case of droplet size and PDI analysis, indicating that the parameters exhibited significant differences in droplet size and PDI of FLU-D NEs. The representative 3D graphs outlined in Figs. 3 and 4 represent the effect of the selected parameters on droplet size and PDI of FLU-D NEs. With respect to the observed parameters, the cosurfactant amount was found to have a significant influence on the droplet size and PDI of FLU-D NE ($p < 0.05$). The results showed that an increase in the cosurfactant amount resulted in a decrease in droplet size and PDI. This might be due to the use of a single surfactant, which is less likely to reduce the interfacial tension between the oily and aqueous phases. Cosurfactants are usually used for further reduction of the fluidity of the interface and thereby increase the entropy of the entire colloidal system [47]. In terms of the SOR, there were insignificant effects on droplet size ($p = 0.699$) and PDI ($p = 0.177$) within the selected range (0.1–0.3). One of the considerations in formulating NE is that the SOR should not be >0.5, as exceeding this ratio might increase the droplet size [61]. The effect of sonication time on droplet size and PDI was also investigated. Increasing the sonication time from 5 min to 15 min had an insignificant effect ($p > 0.05$) on both dependent variables, thus indicating that sonication for 5 min was enough time to produce droplets within the nano range. The amount of oil used in the NE had a significant effect ($p = 0.01$) on the droplet size and PDI ($p = 0.3$). The goals for selecting the optimum formula were minimum droplet size, PDI, oil amount and sonication time. Several formulations were generated by the software and were ranked based on the desirability factor. The formulation with

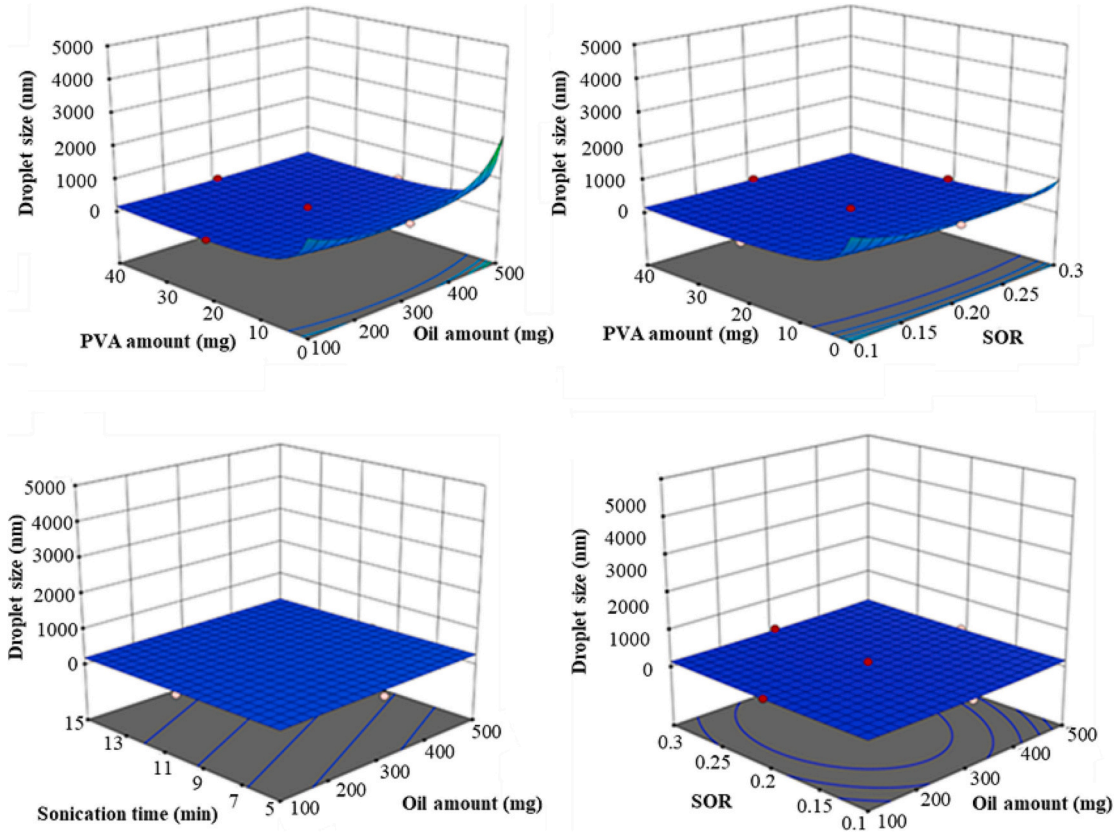

Fig. 3. Response surface plots describing the effect of formulation parameters on the droplet size of FLU-D NE.

the highest desirability was chosen and formulated in triplicate to record the means of the responses. The results showed that the droplet size of the optimised FLU-D NE was 186.34 ± 1.6 nm, with a PDI of 0.147 ± 0.009.

As the final formulation of this NE is to be loaded into the MN formulation, increasing the drug amount in the NE was needed. The effect of increasing drug loading on the droplet size and PDI of the optimised FLU-D NE was investigated using DLS. Fig. 5 **(A)** and **(B)** show the droplet size and PDI of the optimised NE upon a gradual increase in the drug amount. Increasing the drug amount from 200 mg to 800 mg did not significantly affect the droplet size of NE ($p = 0.177$), while the PDI in both NEs was <0.3, which indicated the narrow size distribution of the droplets. TEM was used to assess the impact of increasing the FLU-D amount from 200 mg to 800 mg on droplet morphology. As demonstrated in Fig. 5 **(C)** and **(D)**, in both cases, FLU-D NE had spherical droplets, and increasing the drug amount to 800 mg did not affect the uniformity or droplet morphology of FLU-D NE. The final FLU-D NE had 800 mg of FLU—D, 100 mg sesame oil and 10 mg Pluronic PL®64 in the oily phase. The aqueous phase contained 20 % *w*/w PVA 10 KDa as cosurfactant.

3.2. Characterisation, release and stability of the optimised FLU-D NE

The stability of the optimised FLU-D NE was studied in terms of droplet size and PDI over a period of two weeks at RT and 4 °C. FLU-D NE showed a high stability in terms of droplet size and PDI without any sign of sedimentation or droplet aggregation. PDI is an indicator of the distribution of droplet sizes, and low PDI values estimate a narrow size distribution. The narrow size distribution leads to higher stability. The PDI values for monodisperse systems can range from 0.05 to 0.7. In this work, a PDI of 0.3 or less was considered an indication for a narrow size distribution and high physical stability [53,64]. The NE have shown good physical stability over the period of the study. NEs are known for having physical stability which is achieved due to adding surfactant or a mixture of surfactant and cosurfactant [36,58]. The oily nanodroplets of the NE were suspended using PL®64 as a surfactant. Further, the stability of the NE was enhanced by using PVA in the aqueous phase of the formulation as a cosurfactant. Adding PVA polymer provided such stability in a previously reported study [36]. Fig. 5 **(E)** and **(F)** show the mean droplet size and PDI of the NE over a period of 14 days of preparation and storage under two different conditions.

The EE% of FLU-D NE was studied using an ultrafiltration technique. A high encapsulation efficiency was detected, with an average of 99.81 ± 0.1 %. This high EE% has been previously reported with NE, as high drug encapsulation enhances bioavailability [65]. Subsequently, the LC % for the optimum FLU-D NE formulation was calculated and found to be 14.5 ± 0.01 % [66]. High LC% values are needed for a formulation to become successful in the clinical setting, since a certain drug concentration has to be reached in the target tissue to provide a therapeutic effect [67]. The *in vitro* release profiles of FLU-D from NE and pure drug are shown in Fig. 5 **(G)**. The *in vitro* release of FLU-D from NE and pure drug continued over 60 days, which indicated their slow diffusion into the aqueous release media despite maintaining sink conditions. FLU-D release from NE over one week was 6.14 ± 3.09 %, whereas for the pure formulation, it was 0.89 ± 0.39 %. After one month of the study, 19.66 ± 10.29 % FLU-D was released from NE, and 1.09 ± 0.60 % FLU-D was detected in release media from the pure drug formulation. There was an increase in the FLU-D amount released from NE and pure drug to be 30.89 ± 7.63 % and 10.73 ± 2.94 %, respectively, following 60 days of the study, which is equivalent to 10.81 ± 6.17 mg and 3.75 ± 4.5 mg FLU—D. This enhancement in the dissolution rate and drug release of the NE compared to the pure drug could be due to the small droplet size of the NE. Reducing the droplet size increases the surface area, which enhances the dissolution rate [68].

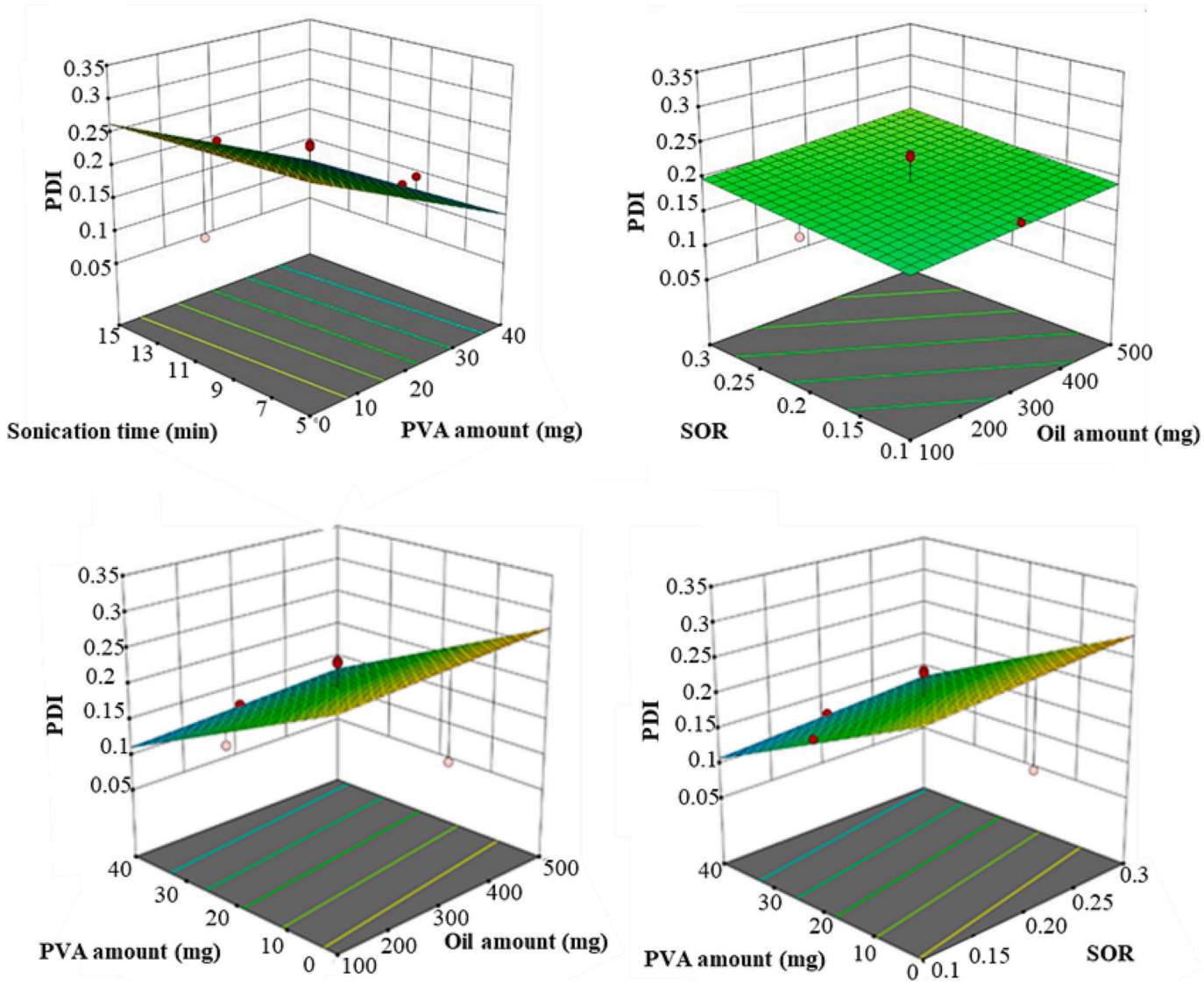

Fig. 4. Response surface plots describing the effect of formulation parameters on the PDI of FLU-D NE.

3.3. MN formulations

FLU-D NE was formulated in the presence of PVA, which has been used extensively for MN formulations [69,70]. To enhance the mechanical properties of the NE, PVP was added to the NE and mixed. FLU-D NE-loaded MNs were fully formed, as shown in Fig. 6 **(A)**. For FLU-D dissolving MNs, the aqueous blend of PVA and PVP has been extensively used in MN formulations, and it has been reported that this polymeric mixture enhanced the mechanical properties of each polymer alone. This enhancement might be explained by the potential formation of hydrogen bonds between the hydroxyl group (-OH) in PVA and the carbonyl group (C=O) in PVP [15]. FLU-D was loaded into the F2 formulation, as it indicated promising mechanical properties. A full formulation of FLU-D-loaded MNs was observed, as shown in Fig. 6 **(B).** Finally, FLU-PLGA tipped MNs were prepared using the multicasting technique. MNs were visualised using a light microscope and evaluated in terms of their mechanical strength, insertion properties and drug content, as outlined in the following sections. Fig. 6 **(C)** shows light microscope images of FLU-PLGA tipped MNs, and Nile red was added to the PLGA tips.

3.4. Mechanical and insertion properties evaluation of the three MN systems

For FLU-D NE-loaded MNs, the outlined results in Fig. 6 **(D)** show that upon conducting the Parafilm®M insertion test, FLU-D NE-loaded MNs penetrated into the second layer of Parafilm®M by >90 %. Each layer of Parafilm®M has a thickness of 126 μm; therefore, the insertion of this MN system is equivalent to 252 μm. MN insertion into the skin is highly important, as they should pass the *stratum corneum (SC)*, which has a thickness of 10–20 μm [71,72]. In terms of the mechanical evaluation, FLU-D NE-loaded MNs had a percentage of height reduction <10 % of the original MN length, as shown in Fig. 6 **(E).** MNs with the same percentage of height reduction approved their ability to penetrate the skin without any mechanical failure, as reported previously [43].

The same evaluations were carried out on FLU-D loaded dissolving MNs, which had a height reduction of 9.8 ± 3.4 %. This result is also similar to previously reported data for drug loaded into dissolving MNs [73]. The FLU-D loaded dissolving MNs were able to reach the third layer of Parafilm®M upon applying 32 N for 30 s, which represents an insertion depth of 378 μm as the mean thickness of each single layer of the Parafilm®M is 126 μm. This result is similar to previously reported insertion studies that demonstrated the ability of MNs to be inserted into

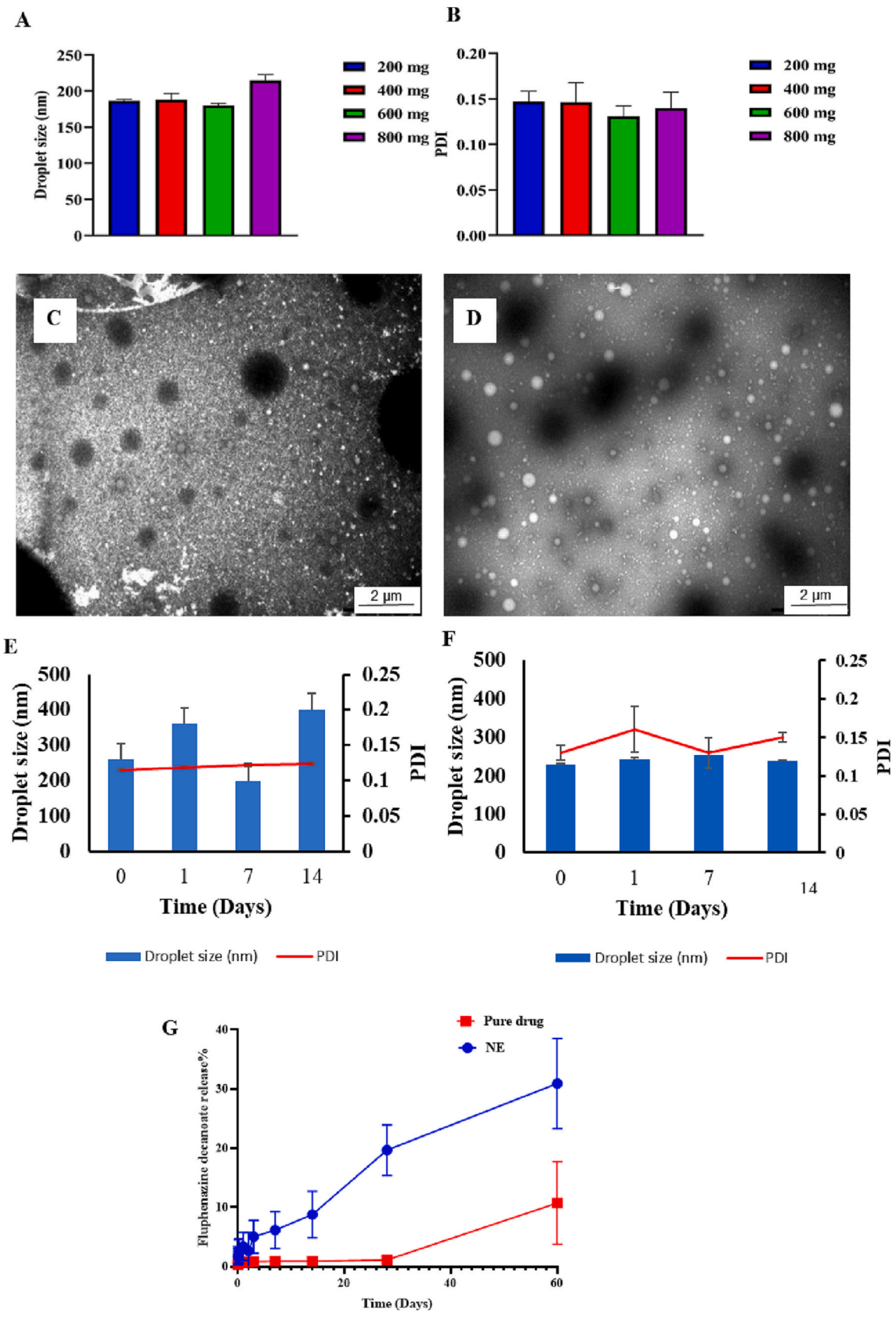

Fig. 5. **A**: The effect of increasing drug loading on the droplet size of NE (means ± S. D, $n = 3$). **B:** The effect of increasing drug loading on the PDI of NE (means ± S·D., n = 3), **C:** TEM image of FLU-D NE prepared with 200 mg of FLU—D. **D:** TEM image of FLU-D NE prepared with 800 mg of FLU—D. **E:** Physical stability of FLU-D NE in terms of droplet size and PDI at RT over 14 days (means ± S.D., n = 3), **F**: The stability of FLU-D NE in terms of maintaining droplet size and PDI at 4 °C over 14 days (means ± S.D., n = 3). **G:** Dialysis bag *in vitro* release of FLU-D from NE compared to pure FLU-D (means ± S. D, n = 3).

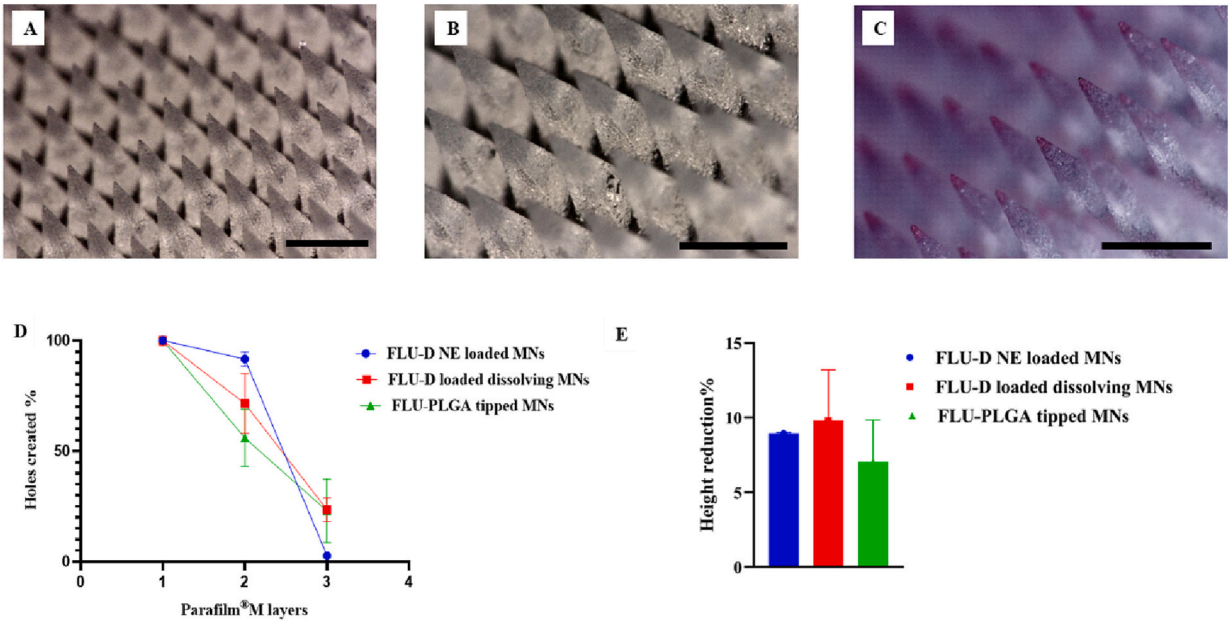

Fig. 6. Light microscope images of **A:** FLU-D NE loaded into dissolving MNs. **B:** FLU-D loaded dissolving MNs **C:** FLU-PLGA tipped MNs. Physical evaluation of the three developed MN systems. **D:** The percentage of the holes created in Parafilm®M upon performing the Parafilm®M insertion test on FLU-D NE-loaded MNs, FLU-D-loaded dissolving MNs and FLU-PLGA-tipped MNs (mean ± SD, $n = 3$). **E:** The percentage of height reduction of FLU-D NE loaded MNs, FLU-D loaded dissolving and FLU-PLGA tipped MNs, (mean + SD, $n = 3$) after applying a force of 32 N for 30 s in compression mood againts an aluminium solid surface.

the skin [74]. Moreover, a compression force test was applied to FLU-PLGA-tipped MNs. Upon applying the test FLU-PLGA tipped MNs showed a percentage of height reduction of 8.04 ± 3.8 %. FLU-PLGA tipped MNs were evaluated in terms of the insertion properties based on the Parafilm®M insertion test. MNs were able to penetrate the third layer of Parafilm®M as well. The insertion and height reduction results of the MN containing NE are in line with the results reported for MNs loaded with nanosuspensions showing height reductions lower than 10 % of the initial height and insertions reaching the 3rd layer of the Parafilm skin simulant [61]. On the other hand, FLU-PLGA-tipped MNs showed a lower height reduction than previously reported PLGA-tipped MN arrays while displaying similar insertion profiles [75].

3.5. FLU in vitro release from FLU-PLGA tipped MNs

The *in vitro* release profile of FLU from the PLGA tips is shown in Fig. 7 **(A).** The release profile of FLU showed that it was released from the PLGA tips over 21 days in the selected release media (0.1 % *w*/w BSA and 1 % w/w SLS in PBS). After 24 h, 193.06 ± 75.90 μg FLU, representing 27.80 ± 9.44 % of the loaded FLU, was released, whereas 441.52 ± 128.15 μg FLU, representing 77.45 ± 22.48 % of the loaded FLU, was released after 7 days. On day 21 of the release study, 512.53 ± 229.95 μg FLU, representing 89.91 ± 40.34 % of the loaded FLU, was released into the release media. This release pattern was similar to that of a previously reported PLGA-tipped MN system. Drug release started with a burst release and extended over three weeks [75]. These results may indicate the capability of FLU-PLGA-tipped MNs to sustain the delivery of FLU.

3.6. Ex vivo skin deposition study of the three MN formulations

An *ex vivo* skin deposition study was performed using FLU-D dissolving MNs and full thickness neonatal porcine skin. The study aimed to quantify the FLU-D amounts deposited in the skin after 24 h of MN insertion and the FLU-D amounts permeated into the reservoir compartment after 24 h of MN insertion. FLU-D hydrolysed to FLU, which was detected in the skin and the release media, and 38.103 ± 19.494 μg FLU-D was deposited in the skin, whereas 160.449 ± 196.473 μg FLU was found. In the release media, only FLU was detected (529.361 ± 74.00 μg), as shown in Fig. 7 **(C).** An *ex vivo* skin deposition study was performed to evaluate the feasibility and efficiency of delivering FLU-D using NE-loaded DMNs. It is hypothesised that due to the high lipophilicity of FLU-D NE, an intradermal depot of FLU-D will be formulated following MN dissolution. Esterases are broadly distributed in various parts of the body, including the skin [76]. FLU-D can hydrolyse to its parent form FLU in the presence of esterases, which can take place in various parts of the body, including the administration site, lymphatic system and blood [77]. FLU and FLU-D amounts in skin and release media were quantified, as FLU is considered responsible for the pharmacological activity among other FLU metabolites [78]. After 24 h of MN application into full thickness neonatal porcine skin, 68.80 ± 17.39 μg FLU-D and 76.51 ± 49.69 μg FLU were quantified in skin samples. While 358.22 ± 106.88 μg FLU was detected while FLU-D was not found in release media, the results are outlined in Fig. 7 **(D).** An *ex vivo* skin deposition study using FLU-PLGA tipped MNs on full thickness neonatal porcine skin showed that 256.79 ± 52.94 μg FLU, which represents 51.35 ± 10.58 % of FLU, was deposited in the skin, while 178.60 ± 80.9 μg FLU, which represents 21.29 ± 8.10 % of FLU, was detected in the release media, as demonstrated in Fig. 7 **(E).**

3.7. In vivo evaluation of MN formulations

After 24 h, the patches were removed to evaluate if the formulation successfully deposited the drug loaded tips into the skin of the animals. Complete dissolving and implantation of all MN formulations were observed. Furthermore, the BPs of the three MN formulations were completely dissolved. Polymer residuals were easily removed with a wet cloth. No erythema or skin abnormality was observed.

This study was designed to examine the delivery of FLU into the systemic circulation using the three developed polymeric MN systems. FLU plasma level profiles of the three MN systems were investigated. Furthermore, FLU plasma levels of the FLU-D loaded dissolving MNs and FLU-D NE loaded MNs were compared to the IM FLU-D oily solution. The FLU plasma levels of FLU-PLGA tipped MNs were compared to those of the oral FLU aqueous solution. The phrase “therapeutic levels” was used for FLU plasma drug concentrations in the range of 1–10 ng/ml, which is

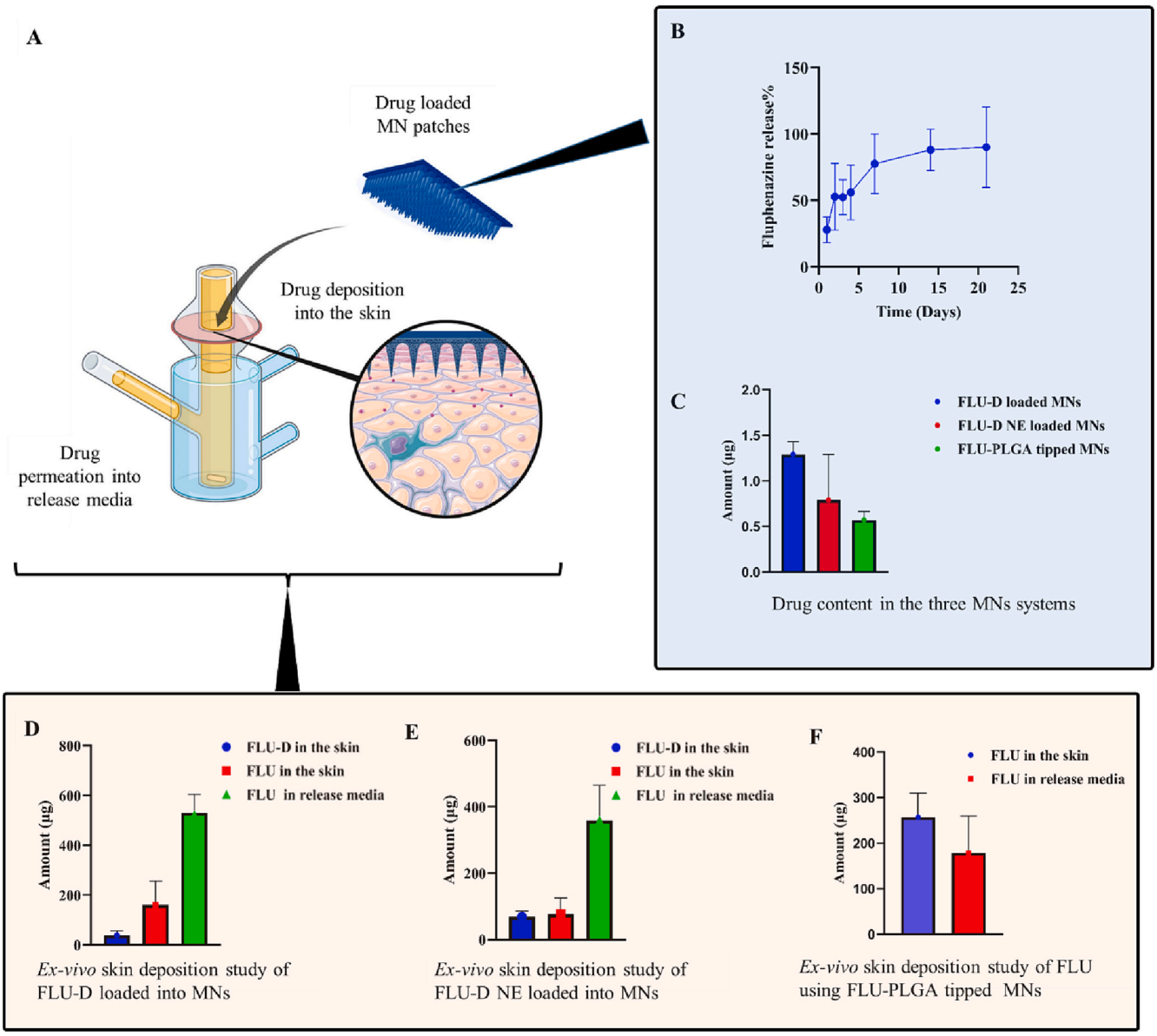

Fig. 7. **A** Schematic illustrating the delivery FLU/FLU-D using MN patches. **B:** The percentage of FLU released from FLU-PLGA tipped MNs into the release media in the *in vitro* release study (mean ± SD, $n = 4$). **C:** Drug content in each of the developed MNs systems (mean ± SD, $n = 4$). **D:** FLU and FLU-D amounts in the skin and release media after performing *ex vivo* skin deposition study on full thickness neonatal porcine skin using FLU-D loaded dissolving MNs (mean ± SD, $n = 4$). **E:** FLU and FLU-D amounts in the skin and release media after performing *ex vivo* skin deposition study on full thickness neonatal porcine skin using FLU-D NE loaded dissolving MNs (mean ± SD, $n = 4$). **F:** FLU amounts in the skin and release media after performing *ex vivo* skin deposition study on full thickness neonatal porcine skin using FLU-PLGA tipped MNs (mean ± SD, $n = 4$).

Table 1
The pharmacokinetic parameters of FLU delivered using FLU-D dissolving microneedles, FLU-D nanoemulsion loaded microneedles, IM of FLU-D in sesame oil or an oral solution of FLU (means ± SD, n = 4).

Group	Dose (mg/kg)	Cmax (ng/ml)	tmax (day)	t ½ (day)	MRT (day)	AUC (ng/ml*d)	Relative bioavailability% (Compared to the IM)
IM FLU-D	5	9.14 ± 1.3	0.16	12.80	9.39 ± 6.4	53.21 ± 33.8	–
FLU-D Dissolving MNs	20.64	36.11 ± 12.37	0.04	3.80	7.6 ± 2.45	59.23 ± 17.57	26.96 %
FLU-D NE loaded MNs	12.64	12.92 ± 6.3	0.04	3.63	6.42 ± 0.45	29.24 ± 2.66	21.73 %
Oral FLU solution	5	41.66 ± 10.49	0.04	0.28	0.40 ± 0.02	20.14 ± 2.05	–
FLU-PLGA tipped MNs	9.12	21.57 ± 2.45	0.04	6.96	9.05 ± 0.61	41.20 ± 6.04	42.45 %

generally accepted as the therapeutic window of FLU [79]. FLU concentration levels in plasma were analysed using the validated *in vivo* high HPLC–MS method. A pharmacokinetic study is an investigation of the movements or kinetics of the drug into, through and out of the body [80]. Several pharmacokinetic principles were investigated in these FLU plasma profiles, namely, C_{max}, t_{max}, $AUC_{(0-7)}$, and half-life ($t_{1/2}$). FLU plasma levels were evaluated following the administration of an aqueous solution of FLU in deionised water, and a dose of 5 mg/kg was given to each rat in the group.

FLU human therapeutic plasma levels were reached within 25 min following the oral administration of FLU solution, and a C_{max} of 41.66 ± 10.49 ng/ml was reached within 1 h, as detailed in Table 1 and Fig. 8 (F). The $AUC_{(0-7)}$ for the oral FLU was 20.14 ± 2.05 ng/ml*d. In a previously reported *in vivo* study investigating the distribution of FLU in rats, a dose of 5 mg/kg of FLU oral solution was given daily to the rats for 15 days. FLU plasma levels were quantified using a radioimmunoassay method, where FLU plasma levels following 6 h of the last oral dose were found to be approximately 98 ± 53 ng/ml. This difference between the values

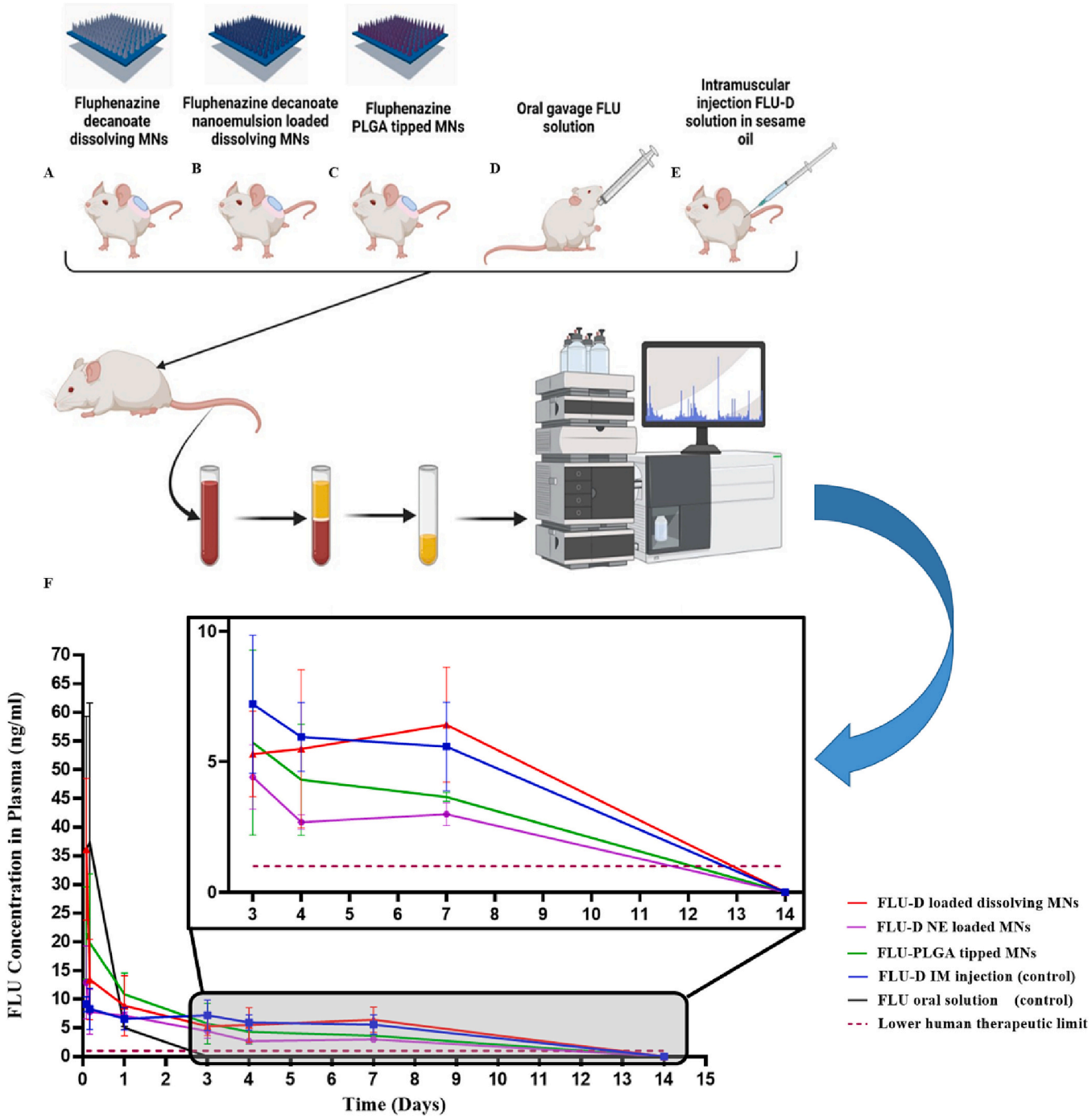

Fig. 8. A schematic representation showing the five groups of the *in vivo* study of **A:** FLU-D dissolving MNs, **B:** FLU-D NE MNs, **C:** FLU-PLGA tipped MNs. **D:** Oral FLU solution, **E:** IM of FLU-D solution in sesame oil. **F:** FLU extraction from plasma samples and analysis using HPLC–MS. **F:** Fluphenazine (FLU) plasma levels [ng/ml] in female Sprague Dawley rats after intramuscular (IM) injection of 5 mg/kg FLU-D in sesame oil, the application of FLU-D loaded DMNs (20.64 mg/kg), (means + SD, $n = 4$), the application of FLU-D NE MNs (12.64 mg/kg), (means + SD, $n = 4$), after oral administration of 5 mg/kg FLU (means + SD, $n = 4$) or the application of FLU-PLGA tipped MNs (9.12 mg/kg) (means + SD, $n = 4$).

reported in our study and their study may be due to drug accumulation after the daily oral administration of FLU for 15 days, as blood samples were analysed following 15 days of daily FLU oral intake [78]. FLU plasma levels and pharmacokinetic parameters were evaluated following the administration of the IM injection of FLU-D in sesame oil solution at a dose of 5 mg/kg. In a previously reported study, 78 mg/kg of FLU-D where intramuscularly injected into 16 rats, on day 7 of the study two rats were died. In this study,the dose of IM FLU-D was chosen to ensure a high level of safety for the rats. FLU therapeutic levels were reached within 4 h of administration and maintained for over a week. The C_{max} was 9.14 ± 1.34 ng/ml, and the t_{max} was 4 h. The $AUC_{(0–7)}$ for the IM control was 53.21 ± 33.8 ng/ml*d. There is limited knowledge regarding the pharmacokinetics of the IM injection of FLU—D. However, a study was carried out to assess the FLU plasma levels in rats following the IM injection of FLU—D. The rats were given a dose of 78 mg/kg (19.5 mg/rat) FLU-D as an IM injection [50]. FLU plasma levels were quantified using the HPLC analytical method at predetermined time points (1, 7, 15 and 32 days). FLU plasma levels were approximately 10 ng/ml on day 1 and declined to approximately 9 ng/ml on day 32 of the study. It was reported that two rats in the study died on day 7. The dose used in our study was approximately 15-fold less than the dose used in the study to avoid any possible adverse effects. FLU human therapeutic plasma levels following the application of FLU-D dissolving MNs were achieved within 1 h following the application and were maintained for a week. The C_{max} was 36.11 ± 12.37 ng/ml and was reached at 1 h, as shown in Fig. 8 (F). The higher C_{max} following the application of MNs than the IM injection administration was also reported in another study, where a nanosuspension of rilpivirine was loaded into dissolving MNs, and the formulation was assessed in terms of the *in vivo* delivery. The pharmacokinetic study was carried out in rats, and the *in vivo* delivery of rilpivirine using IM was compared to that using MNs. MNs showed a similar pharmacokinetic profile compared to the IM injection of rilpivirine nanosuspension, with higher C_{max} than the IM injection [81].

For the dissolving MNs, the $AUC_{(0–7)}$ was 59.23 ± 17.57 ng/ml*d. AUC is commonly used to indicate the exposure of the drug in the body [82]. The relative bioavailability of FLU delivered using dissolving MNs compared to the IM control was 26.96 %. FLU-D NE loaded dissolving MNs group achieved the therapeutic level of FLU following 1 h of MNs application and maintained for a week, as for the IM control. The C_{max} was 12.92 ± 6.3 ng/ml and was achieved at 1 h following MN application, as outlined in Fig. 8 (F). The $AUC_{(0–7)}$ was 29.24 ± 2.66 ng/ml*d, and the relative bioavailability compared to the IM control was 21.73 %. These findings indicated the potential suitability of combining NE with MNs for delivering and sustaining the delivery of poorly water-soluble drugs. The results of this study were in agreement with a previous study reporting a delivery system of MNs combined with a lipidic nanocarrier. Solid lipid nanoparticles were loaded into dissolving MNs and evaluated as an intradermal delivery system using a rat model. The AUC value of solid lipid nanoparticles loaded into dissolving MNs was significantly higher than that of the oral control group [83]. For FLU-PLGA tipped MNs, the C_{max} was 21.57 ± 2.45 ng/ml and t_{max} was 1 h, while the $AUC_{(0–7)}$ was 41.20 ± 6.04 ng/ml*d and the relative bioavailability compared to the IM control was 42.45 %, as detailed in Table 1.

The three investigated MN systems maintained FLU plasma levels, as did the IM control, over a week, above the lower human plasma therapeutic limit of FLU. The $AUC_{(0–7)}$ of the IM was compared to the $AUC_{(0–7)}$ of the dissolving MNs using the Mann–Whitney test, which indicated an insignificant difference between the 2 values ($p = 0.34$). The same test was applied to compare the AUC of the IM to the $AUC_{(0–7)}$ of NE-loaded MNs, which indicated a significant difference between the 2 values ($p = 0.028$). The difference between the $AUC_{(0–7)}$ of the dissolving MNs and the NE loaded MNs was also compared using the same test, and the result also indicated a significant difference ($p = 0.028$). The $AUC_{(0–7)}$ obtained following the application of FLU-PLGA tipped MNs was not significantly different ($p = 0.8857$) from the $AUC_{(0–7)}$ of the IM control.

The relative bioavailability of FLU delivered from dissolving MNs was higher than that delivered from NE loaded MNs, as detailed in Table 1. These findings might be related to the difference in the drug loading between each of the developed MN systems. FLU-PLGA tipped MNs showed better relative bioavailability than the IM control. In terms of the MRT values, the difference in the MRT between FLU-D dissolving MNs, FLU-D NE MNs and FLU-PLGA tipped MNs compared to the IM control was insignificant ($p = 0.699$, $p = 0.588$ and $p = 0.8857$, respectively). These findings suggested a relatively similar residency time of the drug delivered by the IM injection or by the three developed MN systems.

The FLU-loaded MN systems reported in this work showed their capability to provide therapeutic drug levels over periods of time comparable to those obtained from IM injection. This suggests that long-acting FLU-D can be administered using MN arrays in an efficient way while avoiding the use of needles or syringes. DMNs proved their ability to deposit antipsychotics in the viable skin layers higher than the *SC* [84]. Additionally, in previous work, MNs were able to sustain the release while providing efficient brain delivery of antipsychotics [85]. Most of the reported antipsychotics NE were delivered through the intranasal, parenteral or oral route of administration [86,87]. Transdermal antipsychotic formulations were mostly reported in research with permeation enhancers, solid lipid nanoparticles, cyclodextrin-drug complex and other delivery systems. This is mostly due to the need for overcoming the *SC* or enhancing the permeation through it [10]. The outcomes of this research highlight the feasibility and suitability of MN technology to provide long-acting delivery. The MN array administration does not require the intervention of healthcare professionals [88]. Therefore, patients can self-administer a FLU or FLU-D-loaded patch. This contributes to alleviating the pressure on healthcare systems while potentially reducing treatment cost [89] Moreover, dissolving MN arrays does not generate sharp wastes that could be potentially problematic [90,91].

4. Conclusion

In this work, three MN systems were developed to deliver FLU into the systemic circulation and to sustain the release over a period of time. FLU-D was formulated as a NE, where the formulation was optimised using CCD. FLU-D NE was prepared using sesame oil as the carrier oil and PL®64 and PVA as surfactants and cosurfactants respectively. The optimised NE had a droplet size <250 nm with a uniform size distribution. The optimised NE was loaded into PVP to form MNs. The second MN system was pure FLU-D loaded into a dissolving MN formulation. Moreover, FLU-PLGA tipped MNs were formulated by casting FLU-PLGA solution to form the tips of the MNs. MNs were able to penetrate the *SC* and deliver the drug to the systemic circulation. Additionally, the three developed MN systems were able to sustain the delivery of FLU for over a week, above the lower human plasma therapeutic limit. MN technology has been proven to be a highly promising approach for delivering poorly water-soluble compounds, as has been shown in this study. Moreover, MN systems have the ability to sustain the release of compounds, such as FLU, by adjusting the type or composition of the polymeric matrix, thus reducing the frequency of administration and ultimately increasing patient compliance. Among the three reported MNs system in this work, FLU-D-DMNs might be the most straightforward MNs formulation. With this formulation, the lipophilicity of the prodrug FLU-D played the major role in sustaining the release. This formulation might represent an ideal approach for such lipophilic molecules. NE-loaded MNs might highly enhance the transdermal delivery of NE. This delivery system would be beneficial for previously reported NEs for several applications. FLU-PLGA tipped MNs is an attractive alternative for conventional implants, forming micro implants array instead of having a single implant with several cm length [92]. The latter requires surgical administration or removal which presents an extra burden in the treatment plan. The MNs systems presented in this work could be further studied in terms of

in vivo biocompatibility and pharmacodynamically to evaluate their pharmacological action and safety using animal model. For future aspects, several considerations must be addressed relating MNs commercialisation and large-scale production. The policies and regulations regarding MNs production should be acknowledged and agreed upon by the regulatory bodies.

CRediT authorship contribution statement

Juhaina M. Abu Ershaid: Investigation, Methodology, Formal analysis, Writing – original draft, Writing – review & editing. **Lalitkumar K. Vora:** Supervision, Investigation, Methodology, Formal analysis, Resources, Writing – review & editing. **Fabiana Volpe-Zanutto:** Investigation, Methodology, Resources, Formal analysis, Writing – review & editing. **Akmal H. Sabri:** Investigation, Methodology, Formal analysis, Writing – review & editing. **Ke Peng:** Investigation, Methodology, Formal analysis, Writing – review & editing. **Qonita K. Anjani:** Investigation, Methodology, Formal analysis, Writing – review & editing. **Peter E. McKenna:** Investigation, Formal analysis, Writing – review & editing. **Anastasia Ripolin:** Formal analysis, Writing – review & editing. **Eneko Larrañeta:** Investigation, Methodology, Formal analysis. **Helen O. McCarthy:** Investigation, Methodology, Resources, Formal analysis. **Ryan F. Donnelly:** Supervision, Investigation, Methodology, Formal analysis, Resources, Funding acquisition, Writing – review & editing.

Declaration of competing interest

Ryan Donnelly is an inventor of patents that have been licenced to companies developing microneedle-based products and is a paid advisor to companies developing microneedle-based products. The resulting potential conflict of interest has been disclosed and is managed by Queen's University Belfast. The companies had no role in the design of the present studies, in the collection, analyses or interpretation of the data, in the writing of the manuscript or in the decision to publish the work.

Other all authors declare that they have no known competing financial interests or personal relationships that could have appeared to influence the work reported in this paper.

Data availability

Data will be made available on request.

Appendix A. Supplementary data

Supplementary data to this article can be found online at https://doi.org/10.1016/j.bioadv.2023.213526.

References

[1] M. Rubinov, E. Bullmore, Schizophrenia and abnormal brain network hubs, Dialogues Clin. Neurosci. 15 (2013) 339–349.
[2] A. Jablensky, The diagnostic concept of schizophrenia: its history, evolution, and future prospects, Dialogues Clin. Neurosci. 12 (2010) 271–287.
[3] H.Y. Chong, Global economic burden of schizophrenia: a systematic review, Neuropsychiatr. Dis. Treat. 12 (2016) 357–373.
[4] E.R. Walker, R.E. Mcgee, B.G. Druss, Mortality in mental disorders and global disease burden implications: a systematic review and meta-analysis, JAMA Psychiatry 72 (2015) 334–341.
[5] A.F. Lehman, Practice guideline for the treatment of patients with schizophrenia, second edition, Am. J. Psychiatry 161 (2004) 1–56.
[6] C.J. Picco, 3d-printed implantable devices with biodegradable rate-controlling membrane for sustained delivery of hydrophobic drugs, Drug Deliv. 29 (2022) 1038–1048.
[7] K. Higashi, Medication adherence in schizophrenia: factors influencing adherence and consequences of nonadherence, a systematic literature review, Ther. Adv. Psychopharmacol. 3 (2013) 200–218.
[8] S. Almond, Relapse in schizophrenia: costs, clinical outcomes and quality of life, Br. J. Psychiatry 184 (2004) 346–351.
[9] M. Pennington, P. Mccrone, The cost of relapse in schizophrenia, PharmacoEconomics 35 (2017) 921–936.
[10] A. Abruzzo, Transdermal delivery of antipsychotics: rationale and current status, CNS Drugs 33 (2019) 849–865.
[11] A.B. Jindal, A.R. Bhide, S. Salave, D. Rana, D. Benival, Long-acting parenteral drug delivery systems for the treatment of chronic diseases, Adv. Drug Deliv. Rev. 198 (2023), 114862, https://doi.org/10.1016/j.addr.2023.114862.
[12] L. Vora, S.V. G., P. Vavia, Zero order controlled release delivery of cholecalciferol from injectable biodegradable microsphere: in-vitro characterization and in-vivo pharmacokinetic studies, Eur. J. Pharm. Sci. 107 (2017) 78–86, https://doi.org/10.1016/j.ejps.2017.06.027.
[13] M.A. Pawar, L.K. Vora, P. Kompella, V.K. Pokuri, P.R. Vavia, Long-acting microspheres of human chorionic gonadotropin hormone: in-vitro and in-vivo evaluation, Int. J. Pharm. 611 (2022), 121312, https://doi.org/10.1016/j.ijpharm.2021.121312.
[14] K. Moffatt, I.A. Tekko, L. Vora, F. Volpe-Zanutto, A.R.J. Hutton, J. Mistilis, C. Jarrahian, N. Akhavein, A.D. Weber, H.O. McCarthy, R.F. Donnelly, Development and evaluation of dissolving microarray patches for co-administered and repeated intradermal delivery of long-acting rilpivirine and cabotegravir nanosuspensions for paediatric HIV antiretroviral therapy, Pharm. Res. (2022), https://doi.org/10.1007/s11095-022-03408-6.
[15] I.A. Tekko, L.K. Vora, F. Volpe-Zanutto, K. Moffatt, C. Jarrahian, H.O. McCarthy, R. F. Donnelly, Novel bilayer microarray patch-assisted long-acting micro-depot cabotegravir intradermal delivery for HIV pre-exposure prophylaxis, Adv. Funct. Mater. 2106999 (2021).
[16] Y. Tomita, Prediction of corresponding dose of transdermal blonanserin to oral dose based on dopamine d2 receptor occupancy: unique characteristics of blonanserin transdermal patch, J. Clin. Psychopharmacol. 42 (2022) 260–269.
[17] E. Larrañeta, L. Vora, Delivery of nanomedicines using microneedles, in: Microneedles for Drug and Vaccine Delivery and Patient Monitoring., 2018, pp. 177–205.
[18] J. Abuershaid, L.K. Vora, R.F. Donnelly, Novel fluphenazine decanoate nanoemulsion loaded dissolving microneedles for transdermal delivery, in: Proceedings of the Controlled Release Society Virtual Annual Meeting, 2021.
[19] M. May, Why drug delivery is the key to new medicines, Nat. Med. 28 (2022) 1100–1102.
[20] E. McAlister, B. Dutton, L.K. Vora, L. Zhao, A. Ripolin, D.S.Z.B.P.H. Zahari, H. L. Quinn, I.A. Tekko, A.J. Courtenay, S.A. Kelly, A.M. Rodgers, L. Steiner, G. Levin, E. Levy-Nissenbaum, N. Shterman, H.O. McCarthy, R.F. Donnelly, Directly compressed tablets: a novel drug-containing reservoir combined with hydrogel-forming microneedle arrays for transdermal drug delivery, Adv. Healthc. Mater. 10 (2021) 2001256, https://doi.org/10.1002/adhm.202001256.
[21] S. Demartis, Q.K. Anjani, F. Volpe-Zanutto, A.J. Paredes, S.A. Jahan, L.K. Vora, R. F. Donnelly, E. Gavini, Trilayer dissolving polymeric microneedle array loading Rose Bengal transfersomes as a novel adjuvant in early-stage cutaneous melanoma management, Int. J. Pharm. 627 (2022), 122217, https://doi.org/10.1016/j.ijpharm.2022.122217.
[22] L.K. Vora, A.J. Courtenay, I.A. Tekko, E. Larrañeta, R.F. Donnelly, Pullulan-based dissolving microneedle arrays for enhanced transdermal delivery of small and large biomolecules, Int. J. Biol. Macromol. 146 (2020) 290–298, https://doi.org/10.1016/j.ijbiomac.2019.12.184.
[23] I.A. Tekko, A.D. Permana, L. Vora, T. Hatahet, H.O. McCarthy, R.F. Donnelly, Localised and sustained intradermal delivery of methotrexate using nanocrystal-loaded microneedle arrays: potential for enhanced treatment of psoriasis, Eur. J. Pharm. Sci. 152 (2020), 105469, https://doi.org/10.1016/j.ejps.2020.105469.
[24] L.K. Vora, K. Moffatt, I.A. Tekko, A.J. Paredes, F. Volpe-Zanutto, D. Mishra, K. Peng, R.R.S. Thakur, R.F. Donnelly, Microneedle array systems for long-acting drug delivery, Eur. J. Pharm. Biopharm. 159 (2021) 44–76, https://doi.org/10.1016/j.ejpb.2020.12.006.
[25] Y.A. Naser, I.A. Tekko, L.K. Vora, K. Peng, Q.K. Anjani, B. Greer, C. Elliott, H. O. McCarthy, R.F. Donnelly, Hydrogel-forming microarray patches with solid dispersion reservoirs for transdermal long-acting microdepot delivery of a hydrophobic drug, J. Control. Release 356 (2023) 416–433, https://doi.org/10.1016/j.jconrel.2023.03.003.
[26] A.J. Paredes, A.D. Permana, F. Volpe-Zanutto, M.N. Amir, L.K. Vora, I.A. Tekko, N. Akhavein, A.D. Weber, E. Larrañeta, R.F. Donnelly, Ring inserts as a useful strategy to prepare tip-loaded microneedles for long-acting drug delivery with application in HIV pre-exposure prophylaxis, Mater. Des. 224 (2022), 111416, https://doi.org/10.1016/j.matdes.2022.111416.
[27] K. Peng, L.K. Vora, I.A. Tekko, A.D. Permana, J. Domínguez-Robles, D. Ramadon, P. Chambers, H.O. McCarthy, E. Larrañeta, R.F. Donnelly, Dissolving microneedle patches loaded with amphotericin B microparticles for localised and sustained intradermal delivery: potential for enhanced treatment of cutaneous fungal infections, J. Control. Release 339 (2021) 361–380, https://doi.org/10.1016/j.jconrel.2021.10.001.
[28] Q.K. Anjani, A.D. Permana, Á. Cárcamo-Martínez, J. Domínguez-Robles, I. A. Tekko, E. Larrañeta, L.K. Vora, D. Ramadon, R.F. Donnelly, Versatility of hydrogel-forming microneedles in in vitro transdermal delivery of tuberculosis drugs, Eur. J. Pharm. Biopharm. 158 (2021) 294–312, https://doi.org/10.1016/j.ejpb.2020.12.003.
[29] A.J. Paredes, F. Volpe-Zanutto, A.D. Permana, A.J. Murphy, C.J. Picco, L.K. Vora, J. A. Coulter, R.F. Donnelly, A.D. Permana, A.J. Murphy, C.J. Picco, L.K. Vora, J. A. Coulter, R.F. Donnelly, Novel tip-loaded dissolving and implantable microneedle array patches for sustained release of finasteride, Int. J. Pharm. 606 (2021), 120885, https://doi.org/10.1016/j.ijpharm.2021.120885.

[30] F. Volpe-Zanutto, L.T. Ferreira, A.D. Permana, M. Kirkby, A.J. Paredes, L.K. Vora, A.P. Bonfanti, I. Charlie-Silva, C. Raposo, M.C. Figueiredo, I.M.O. Sousa, A. Brisibe, F.T.M. Costa, R.F. Donnelly, M.A. Foglio, Artemether and lumefantrine dissolving microneedle patches with improved pharmacokinetic performance and antimalarial efficacy in mice infected with Plasmodium yoelii, J. Control. Release 333 (2021) 298–315, https://doi.org/10.1016/j.jconrel.2021.03.036.

[31] B. Pamornpathomkul, T. Ngawhirunpat, I.A. Tekko, L. Vora, H.O. McCarthy, R. F. Donnelly, Dissolving polymeric microneedle arrays for enhanced site-specific acyclovir delivery, Eur. J. Pharm. Sci. 121 (2018) 200–209, https://doi.org/10.1016/j.ejps.2018.05.009.

[32] H. Abd-El-Azim, I.A. Tekko, A. Ali, A. Ramadan, N. Nafee, N. Khalafallah, T. Rahman, W. Mcdaid, R.G. Aly, L.K. Vora, S.J. Bell, F. Furlong, H.O. McCarthy, R. F. Donnelly, Hollow microneedle assisted intradermal delivery of hypericin lipid nanocapsules with light enabled photodynamic therapy against skin cancer, J. Control. Release S0168-3659 (22) (2022), https://doi.org/10.1016/j.jconrel.2022.06.027, 00365–0.

[33] G. Clarke, Fluphenazeve decanoate, in: Analytical Profiles of Drug Substances, Elsevier, 1981, pp. 275–294.

[34] J.-P. Luo, J.W. Hubbard, K.K. Midha, Sensitive method for the simultaneous measurement of fluphenazine decanoate and fluphenazine in plasma by high-performance liquid chromatography with cuolometric detection, J. Chromatogr. B Biomed. Sci. Appl. 688 (1997) 303–308.

[35] I.K. Ramöller, M.T. Abbate, L.K. Vora, A.R. Hutton, K. Peng, F. Volpe-Zanutto, I. A. Tekko, K. Moffatt, A.J. Paredes, H.O. McCarthy, et al., HPLC-MS method for simultaneous quantification of the antiretroviral agents rilpivirine and cabotegravir in rat plasma and tissues, J. Pharm. Biomed. Anal. 213 (2022), 114698.

[36] M.I. Nasiri, Nanoemulsion-based dissolving microneedle arrays for enhanced intradermal and transdermal delivery, Drug Deliv. Transl. Res. 12 (2022) 881–896.

[37] V.P. Chavda, D. Shah, A review on novel emulsification technique: a nanoemulsion, research & reviews, J. Pharmacol. Toxicol. Stud. 5 (2017) 29–38.

[38] Y. Wu, L.K. Vora, Y. Wang, M.F. Adrianto, I.A. Tekko, D. Waite, R.F. Donnelly, R.R. S. Thakur, Long-acting nanoparticle-loaded bilayer microneedles for protein delivery to the posterior segment of the eye, Eur. J. Pharm. Biopharm. 165 (2021) 306–318, https://doi.org/10.1016/j.ejpb.2021.05.022.

[39] Y. Wu, L.K. Vora, D. Mishra, M.F. Adrianto, S. Gade, A.J. Paredes, R.F. Donnelly, T. R.R. Singh, Nanosuspension-loaded dissolving bilayer microneedles for hydrophobic drug delivery to the posterior segment of the eye, Biomater. Adv. 137 (2022), 212767, https://doi.org/10.1016/j.bioadv.2022.212767.

[40] S.A. Stewart, Poly (caprolactone)-based subcutaneous implant for sustained delivery of levothyroxine, Int. J. Pharm. 607 (2021), 121011.

[41] K. Peng, Hydrogel-forming microneedles for rapid and efficient skin deposition of controlled release tip-implants, Mater. Sci. Eng. C 127 (2021), 112226.

[42] S. Abdelghany, I.A. Tekko, L. Vora, E. Larrañeta, A.D. Permana, R.F. Donnelly, Nanosuspension-based dissolving microneedle arrays for intradermal delivery of curcumin, Pharmaceutics. 11 (2019) 308, https://doi.org/10.3390/pharmaceutics11070308.

[43] A.S. Cordeiro, I.A. Tekko, M.H. Jomaa, L. Vora, E. McAlister, F. Volpe-Zanutto, M. Nethery, P.T. Baine, N. Mitchell, D.W. McNeill, R.F. Donnelly, Two-photon polymerisation 3D printing of microneedle array templates with versatile designs: application in the development of polymeric drug delivery systems, Pharm. Res. 37 (2020), https://doi.org/10.1007/s11095-020-02887-9.

[44] Á. Cárcamo-Martínez, B. Mallon, Q.K. Anjani, J. Domínguez-Robles, E. Utomo, L. K. Vora, I.A. Tekko, E. Larrañeta, R.F. Donnelly, Enhancing intradermal delivery of tofacitinib citrate: comparison between powder-loaded hollow microneedle arrays and dissolving microneedle arrays, Int. J. Pharm. 593 (2021), 120152, https://doi.org/10.1016/j.ijpharm.2020.120152.

[45] A.J. Courtenay, E. McAlister, M.T.C. McCrudden, L. Vora, L. Steiner, G. Levin, E. Levy-Nissenbaum, N. Shterman, M.-C. Kearney, H.O. McCarthy, R.F. Donnelly, Hydrogel-forming microneedle arrays as a therapeutic option for transdermal esketamine delivery, J. Control. Release 322 (2020) 177–186, https://doi.org/10.1016/j.jconrel.2020.03.026.

[46] H.E. Matar, M.Q. Almerie, S.J. Sampson, Fluphenazine (oral) versus placebo for schizophrenia, Cochrane Database Syst. Rev. 6 (2018), CD006352.

[47] J.M. Meyer, Understanding depot antipsychotics: an illustrated guide to kinetics, CNS Spectr. 18 (2013) 55–68.

[48] B. Gorain, Nanoemulsion strategy for olmesartan medoxomil improves oral absorption and extended antihypertensive activity in hypertensive rats, Colloids Surf. B: Biointerfaces 115 (2014) 286–294.

[49] Y. Singh, Nanoemulsion: concepts, development and applications in drug delivery, J. Control. Release 252 (2017) 28–49.

[50] Y. Huang, J. Hubbard, K. Midha, The role of the lymphatic system in the presystemic absorption of fluphenazine after intramuscular administration of fluphenazine decanoate in rats, Eur. J. Pharm. Sci. 3 (1995) 15–20.

[51] N.M. Aljabri, N. Shi, A. Cavazos, Nanoemulsion: an emerging technology for oilfield applications between limitations and potentials, J. Pet. Sci. Eng. 208 (2022), 109306.

[52] M.I. Nasiri, L.K. Vora, J.A. Ershaid, K. Peng, I.A. Tekko, R.F. Donnelly, A. Ershaid Juhaina, Ke Peng, I.A. Tekko, R.F. Donnelly, Nanoemulsion-based dissolving microneedle arrays for enhanced intradermal and transdermal delivery, Drug Deliv. Transl. Res. 1 (2021) 3, https://doi.org/10.1007/s13346-021-01107-0.

[53] V.K. Rai, Nanoemulsion as pharmaceutical carrier for dermal and transdermal drug delivery: formulation development, stability issues, basic considerations and applications, J. Control. Release 270 (2018) 203–225.

[54] M. Mahadev, Fabrication and evaluation of quercetin nanoemulsion: a delivery system with improved bioavailability and therapeutic efficacy in diabetes mellitus, Pharmaceuticals 15 (2022) 70.

[55] S. Sharma, Interfacial and colloidal properties of emulsified systems: pharmaceutical and biological perspective, in: Colloid and Interface Science in Pharmaceutical Research and Development, Elsevier, 2014.

[56] F.S. El-Tokhy, Transdermal delivery of second-generation antipsychotics for management of schizophrenia; disease overview, conventional and nanobased drug delivery systems, J. Drug Delivery Sci. Technol. 61 (2021), 102104.

[57] H. Yazgan, Investigation of antimicrobial properties of sage essential oil and its nanoemulsion as antimicrobial agent, LWT 130 (2020), 109669.

[58] V. Bali, M. Ali, J. Ali, Study of surfactant combinations and development of a novel nanoemulsion for minimising variations in bioavailability of ezetimibe, Colloids Surf. B: Biointerfaces 76 (2010) 410–420.

[59] A.A. Abu Sharar, S.Z. Ramadan, S.H. Hussein-Al-Ali, Multiobjective optimization of fluphenazine nanocomposite formulation using nsga-ii method, Mater. Sci.-Pol. 39 (2021) 517–544.

[60] M.M. Dunne, Z. Ramtoola, O.I. Corrigan, Fluphenazine release from biodegradable microparticles: characterization and modelling of release, J. Microencapsul. 26 (2009) 403–410.

[61] L.K. Vora, P.R. Vavia, E. Larrañeta, S.E.J.J. Bell, R.F. Donnelly, Novel nanosuspension-based dissolving microneedle arrays for transdermal delivery of a hydrophobic drug, J. Interdiscip. Nanomed. 3 (2018) 89–101.

[62] D. Chobisa, Design of experiments for the development of injectable drug products, in: S. Beg (Ed.), Design of Experiments for Pharmaceutical Product Development: Volume II : Applications and Practical Case Studies, Springer Singapore, Singapore, 2021, pp. 69–96, https://doi.org/10.1007/978-981-33-4351-1_5.

[64] L. Vora, M. Tyagi, K. Patel, S. Gupta, P. Vavia, Self-assembled nanocomplexes of anionic pullulan and polyallylamine for DNA and pH-sensitive intracellular drug delivery, J. Nanopart. Res. 16 (2014) 1–13.

[65] Z. Zhao, Preparation, characterization, and evaluation of antioxidant activity and bioavailability of a self-nanoemulsifying drug delivery system (snedds) for buckwheat flavonoids, Acta Biochim. Biophys. Sin. Shanghai vol. 52 (2020) 1265–1274.

[66] A. Ramalheiro, Rapidly dissolving microneedles for the delivery of cubosome-like liquid crystalline nanoparticles with sustained release of rapamycin, Int. J. Pharm. 591 (2020), 119942.

[67] D. Khunt, B.G. Prajapati, M. Prajapti, M. Misra, S. Salave, J.K. Patel, R.J. Patel, Drug delivery by Micro, Nanoemulsions in tuberculosis, in: R. Shegokar, Y. Pathak (Eds.), Tubercular Drug Delivery Systems: Advances in Treatment of Infectious Diseases, Springer International Publishing, Cham, 2023, pp. 173–188, https://doi.org/10.1007/978-3-031-14100-3_9.

[68] M. Laxmi, Development and characterization of nanoemulsion as carrier for the enhancement of bioavailability of artemether, Artif. Cells Nanomed. Biotechnol. 43 (2015) 334–344.

[69] A. Himawan, Q.K. Anjani, U. Detamornrat, L.K. Vora, A.D. Permana, R. Ghanma, Y. Naser, D. Rahmawanty, C.J. Scott, R.F. Donnelly, Multifunctional low temperature-cured PVA/PVP/citric acid-based hydrogel forming microarray patches: physicochemical characteristics and hydrophilic drug interaction, Eur. Polym. J. 186 (2023), 111836, https://doi.org/10.1016/j.eurpolymj.2023.111836.

[70] E. Altuntaş, I.A. Tekko, L.K. Vora, N. Kumar, R. Brodsky, O. Chevallier, E. McAlister, Q.K. Anjani, H.O. McCarthy, R.F. Donnelly, Nestorone nanosuspension-loaded dissolving microneedles array patch: a promising novel approach for “on-demand” hormonal female-controlled peritcoital contraception, Int. J. Pharm. 614 (2022), 121422, https://doi.org/10.1016/j.ijpharm.2021.121422.

[71] S. Rojekar, L.K. Vora, I.A. Tekko, F. Volpe-Zanutto, H.O. McCarthy, P.R. Vavia, R. F. Donnelly, Etravirine-loaded dissolving microneedle arrays for long-acting delivery, Eur. J. Pharm. Biopharm. 165 (2021) 41–51, https://doi.org/10.1016/j.ejpb.2021.04.024.

[72] H.S. Faizi, L.K. Vora, M.I. Nasiri, Y. Wu, D. Mishra, Q.K. Anjani, A.J. Paredes, R.R. S. Thakur, M.U. Minhas, R.F. Donnelly, Deferasirox nanosuspension loaded dissolving microneedles for intradermal delivery, Pharmaceutics 14 (2022) 2817.

[73] A. Rein-Weston, I. Tekko, L. Vora, C. Jarrahian, B. Spreen, T. Scott, R. Donnelly, D. Zehrung, LB8., Microarray patch delivery of long-acting HIV PrEP and contraception, in: Open Forum Infectious Diseases, Oxford University Press, 2019, p. S996.

[74] R.E. Lutton, Microneedle characterisation: the need for universal acceptance criteria and gmp specifications when moving towards commercialisation, Drug Deliv. Transl. Res. 5 (2015) 313–331.

[75] K. Peng, L.K. Vora, J. Domínguez-Robles, Y.A. Naser, M. Li, E. Larrañeta, R. F. Donnelly, Hydrogel-forming microneedles for rapid and efficient skin deposition of controlled release tip-implants, Mater. Sci. Eng. C 127 (2021), 112226.

[76] M. Rooseboom, J.N. Commandeur, N.P. Vermeulen, Enzyme-catalyzed activation of anticancer prodrugs, Pharmacol. Rev. 56 (2004) 53–102.

[77] J.-P. Luo, J.W. Hubbard, K.K. Midha, Studies on the mechanism of absorption of depot neuroleptics: fluphenazine decanoate in sesame oil, Pharm. Res. 14 (1997) 1079–1084.

[78] M. Aravagiri, Distribution of fluphenazine and its metabolites in brain regions and other tissues of the rat, Neuropsychopharmacology 13 (1995) 235–247.

[79] S. Siragusa, K.G. Bistas, A. Saadabadi, S. Fluphenazine, StatPearls Publishing, 2022.

[80] S.M. Coulter, S. Pentlavalli, L.K. Vora, Y. An, E.R. Cross, K. Peng, K. McAulay, R. Schweins, R.F. Donnelly, H.O. McCarthy, et al., Enzyme-triggered l-α/d-peptide hydrogels as a long-acting injectable platform for systemic delivery of HIV/AIDS drugs, Adv. Healthcare Mater. (2023), 2203198.

[81] M.T.C.M. Crudden, E. Larrañeta, A. Clark, C. Jarrahian, A. Rein-Weston, S. Lachau-Durand, N. Niemeijer, P. Williams, C. Haeck, H.O. McCarthy, D. Zehrung, R. F. Donnelly, Design, formulation and evaluation of novel dissolving microarray patches containing a long-acting rilpivirine nanosuspension, J. Control. Release 28 (2018) 119–129, https://doi.org/10.1016/j.jconrel.2018.11.002.
[82] J.D. Scheff, Assessment of pharmacologic area under the curve when baselines are variable, Pharm. Res. 28 (2011) 1081–1089.
[83] A.D. Permana, Solid lipid nanoparticle-based dissolving microneedles: a promising intradermal lymph targeting drug delivery system with potential for enhanced treatment of lymphatic filariasis, J. Control. Release 316 (2019) 34–52.
[84] L.K. Vora, K. Moffatt, R.F. Donnelly, Long-lasting drug delivery systems based on microneedles, in: Long-acting Drug Delivery Systems, Woodhead Publishing, 2022, pp. 249–287.
[85] R.S. Bhadale, V.Y. Londhe, A comparison of dissolving microneedles and transdermal film with solid microneedles for iloperidone in vivo: a proof of concept, Naunyn-Schmiedeberg's, Arch. Pharmacol. 396 (2023) 239–246.
[86] P.C. Pires, A.C. Paiva-Santos, F. Veiga, Antipsychotics-loaded nanometric emulsions for brain delivery, Pharmaceutics 14 (2022) 2174.
[87] D.K. Khatri, K. Preeti, S. Tonape, S. Bhattacharjee, M. Patel, S. Shah, P.K. Singh, S. Srivastav, D. Gugulothu, L. Vora, S.B. Singh, Nanotechnological advances for nose to brain delivery of therapeutics to improve the Parkinson therapy, Curr. Neuropharmacol. (2022), https://doi.org/10.2174/1570159x20666220507022701.
[88] Á. Cárcamo-Martínez, B. Mallon, J. Domínguez-Robles, L.K. Vora, Q.K. Anjani, R. F. Donnelly, Hollow microneedles: a perspective in biomedical applications, Int. J. Pharm. 599 (2021), 120455, https://doi.org/10.1016/j.ijpharm.2021.120455.
[89] E. McAlister, M. Kirkby, J. Domínguez-Robles, A.J. Paredes, Q.K. Anjani, K. Moffatt, L.K. Vora, A.R.J. Hutton, P.E. McKenna, E. Larrañeta, R.F. Donnelly, The role of microneedle arrays in drug delivery and patient monitoring to prevent diabetes induced fibrosis, Adv. Drug Deliv. Rev. 175 (2021), 113825, https://doi.org/10.1016/j.addr.2021.06.002.
[90] F. Volpe-Zanutto, L.K. Vora, I.A. Tekko, P.E. McKenna, A.D. Permana, A.H. Sabri, Q.K. Anjani, H.O. McCarthy, A.J. Paredes, R.F. Donnelly, Hydrogel-forming microarray patches with cyclodextrin drug reservoirs for long-acting delivery of poorly soluble cabotegravir sodium for HIV pre-exposure prophylaxis, J. Control. Release 348 (2022) 771–785, https://doi.org/10.1016/j.jconrel.2022.06.028.
[91] I.A. Tekko, G. Chen, J. Domínguez-Robles, R.R.S. Thakur, I.M.N. Hamdan, L. Vora, E. Larrañeta, J.C. McElnay, H.O. McCarthy, M. Rooney, R.F. Donnelly, Development and characterisation of novel poly (vinyl alcohol)/poly (vinyl pyrrolidone)-based hydrogel-forming microneedle arrays for enhanced and sustained transdermal delivery of methotrexate, Int. J. Pharm. 586 (2020), 119580, https://doi.org/10.1016/j.ijpharm.2020.119580.
[92] E. Magill, S. Demartis, E. Gavini, A.D. Permana, R.R.S. Thakur, M.F. Adrianto, D. Waite, K. Glover, C.J. Picco, A. Korelidou, U. Detamornrat, L.K. Vora, L. Li, Q. K. Anjani, R.F. Donnelly, J. Domínguez-Robles, E. Larrañeta, Solid implantable devices for sustained drug delivery, Adv. Drug Deliv. Rev. 199 (2023) 114950, https://doi.org/10.1016/j.addr.2023.114950.
[93] C. Zhang, L.K. Vora, I.A. Tekko, F. Volpe-Zanutto, K. Peng, A.J. Paredes, H. O. McCarthy, R.F. Donnelly, Development of dissolving microneedles for intradermal delivery of the long-acting antiretroviral drug bictegravir, Int. J. Pharm. 642 (2023) 123108, https://doi.org/10.1016/j.ijpharm.2023.123108.